DIAGNOSTIC, CLINICAL AND ULTRASONOGRAPHIC FEATURES OF ABDOMINAL DISEASE CONDITIONS IN DOGS

DR. LILYAN WANJIKU MATHAI, BVM (UON)

A thesis submitted in partial fulfilment of requirements for the award of the degree of Master of Veterinary Surgery of the University of Nairobi.

DEPARTMENT OF CLINICAL STUDIES

FACULTY OF VETERINARY MEDICINE

UNIVERSITY OF NAIROBI

2015

DECLARATION

This thesis is my original work and has not been presented for award of degree in any other University.

Signed.....Date: 18/11/2015

Dr. Lilyan Wanjiku Mathai (BVM)

This thesis is submitted for examination with our approval as University Supervisors:

Signed.....Date: 18/11/2015

Prof. David O. Kihurani (BVM, MSc, PhD)

Signed.....Date: 19/11/2015

Prof. John D. Mande (BVM, MSc, PhD)

DEDICATION

To my parents Mr. Peter Gichangi Mathai and Mrs. Mary Wanjira Mathai for the love and support you have given to me all my years.

In all the world there is no heart for me like yours.

In all the world there is no love for you like mine.

-Maya Angelou

ACKNOWLEDGEMENTS

I acknowledge my supervisors Prof. David Kihurani and Prof. John Mande for their support, encouragement and advice during my project work.

My brothers Michael, Felix and sisters; Patricia and Ann who provided moral and financial support during my studies.

The Department of Clinical Studies, Faculty of Veterinary Medicine and the University of Nairobi which facilitated access to clinical cases, diagnostic laboratories, Xray, Ultrasound and post mortem facilities.

I would like to thank the staff of Small Animal Clinic; Mr. Victor Jumba, Mr. Peter Mugendi, Mr. Charles Maina, Ms. Mary Mukiri for aiding in the preparation and scanning procedures. Mrs. Alice Kinyua, Ms. Jane Kamau and Ms. Jane Onsongo who assisted with analysis of haematological and clinical chemistry samples.

Dr. Ronald Wairagu who assisted in the analysis of my results. Special mention to Dr. Dhaval Shah for his assistance with processing of histopathological samples.

Drs. Silvia Situma, Edwin Mwangi, Peter Kimeli, Vasani, Pauline Gitonga, and Patricia Wasike, for encouraging and assisting me in the course of my study period. I am truly grateful for their friendship and invaluable professional and moral support.

TABLE OF CONTENTS

LIST OF FIGURES

LIST OF TABLES

ABBREVIATIONS AND ACRONYMS

AFAST	abdominal focused assessment with sonography for trauma
AFS	Abdominal fluid score
CBC	Complete Blood Count
CT	Computed Tomography
CUES	Contrast Enhanced Ultrasound
Lk (h)	left kidney horizontal measurement (cm)
Lk (v)	left kidney vertical measurement (cm)
MHz	Mega Hertz
MRI	Magnetic Resonance Imaging
RBC	Red Blood Cell
RTA	Road traffic accidents
Rk (h)	right kidney horizontal measurement (cm)
Rk (v)	right kidney vertical measurement (cm)
SAC	Small Animal Clinic
Swt	Stomach wall thickness measurement (cm)
Sit,	Intestinal wall measurement (cm)
US	Ultrasound
WHO	World Health Organisation

ALT	Alanine aminotransferase
ALP	Alkaline phosphatase
BUN	Blood Urea Nitrogen

DEFINITIONS

Echotexture	the appearance of tissues based on their acoustic impedance
Anechoic	appearance of fluids on an ultrasound scan screen. The fluids appear a dark/black
Hypoechoic	a grey appearance normally seen in tissues with uniform parenchyma
Hyperechoic	a white appearance normally due to highly reflective tissue interfaces such as air and bone.

ABSTRACT

Diagnostic imaging modalities such as radiography, ultrasonography, fluoroscopy, scintigraphy, magnetic resonance imaging and computed tomography have been used in veterinary practice. Ultrasound is a non-invasive imaging modality which uses high frequency sound waves to facilitate visualization of the internal architecture of parenchymatous and viscous organs. Its major advantages over other imaging techniques include the fact that, it is safe, non-invasive, cost effective and easy to perform. Reports and scientific literature on the ultrasonographic evaluation of abdominal disease conditions in dogs in Kenya are scanty. Data on these aspects of diagnostic, clinical and ultrasonographic features of abdominal disease conditions remain limited and thus the information from this study could help in the diagnosis of abdominal disease.

The aim of this study was to enhance the use of ultrasonography as a diagnostic tool in the effective management of abdominal disease conditions in dogs presented at the Small Animal Clinic, University of Nairobi, Kenya (2011-2013). The objectives were to relate the clinical features of abdominal conditions and their ultrasound findings; to compare the ultrasonographic appearance of abdominal organs in normal and diseased dogs; and to determine a confirmatory diagnosis using ultrasound supported by other ancillary tests. These tests included: radiography, haematology and clinical chemistry, abdominal fluid analysis, exploratory laparotomy, post-mortem and histopathological examination.

Organs that were selected for ultrasound scanning included: the liver, spleen, stomach, intestines, uterus in bitches, right and left kidneys and the urinary bladder. The acoustic window used to scan the uterus was the urinary bladder through the ventral midline

body wall. All organs were scanned trans-cutaneously based on their corresponding anatomic locations.

Thirty clinically normal dogs were scanned to serve as a control group and reference for normal tissue appearances. Dogs were evaluated by physical examination and categorized according to body weight and breed types. Investigation comprised twenty five purposively selected dogs which fulfilled the criteria of exhibiting clinical signs of abdominal disease. The abdominal organs of dogs were scanned with the organ of interest being selected as the organ whose pathology had led to the clinical signs exhibited.

The following measurements were recorded for analysis: right kidney horizontal diameters (Rkh), right kidney vertical diameter (Rkv), left kidney horizontal diameters (Lkh), left kidney vertical diameter (Lkv), the stomach wall thickness (Sw) and intestinal wall thickness (Sit). Data was analysed quantitatively using the independent t-test to compare breed types and age groups. The study findings revealed at 95% confidence interval, a significant difference in the left kidney horizontal diameter (Lkh) of large breeds ($p=0.02$) when compared to the right kidney horizontal diameter (Rkh). The p values of the other measurements showed no significant difference ($p>0.05$) between both breed types and age groups.

The sonograms were descriptively evaluated based on changes in echotexture. The control group sonograms were compared with the research group‘s sonograms. It was found that the echotexture of the organs exhibiting pathologies was detectable on ultrasound and the changes varied from mild to severe. The ultrasound findings were related to the clinical features exhibited in the dogs diagnosed with the various abdominal conditions. These included liver cirrhosis, urinary bladder calculi, splenic hemangiosarcoma and pyometra.

Results showed that the liver was viewed with best clarity compared to other organs due to its location and size. The right kidney was often not visualized due to obstruction by air in the overlapping thoracic cavity. The stomach was best visualized when filled with fluid. The urinary bladder was used as an acoustic window to view abdominal organs due to acoustic enhancement property of fluid such as urine. The uterus was visualized only when it was filled with contents such as when it contained pus or foetal parts. The spleen was best visualized on the left caudal border of the last rib. The intestines were not well visualized due to reverberation artefacts due to gas accumulation in the intestinal tract.

Challenges recorded during the study were numerous artefacts seen in the sonograms such as pseudo sludge, reverberation, acoustic enhancement, clean and dirty acoustic shadows. Knowledge of the artefacts and proper ways to compensate for these helped in preventing misdiagnosis.

It was concluded that, whilst the use of ultrasonography has its challenges in the diagnosis of abdominal disease conditions, conditions such as liver cirrhosis and pyometra were easily identified. Prognosis was reached based on pathologic changes in echotexture and other ancillary tests. This varied from case to case.

It was noted that ultrasound proved to be a good diagnostic imaging tool for abdominal disease conditions. Routine ultrasonography is proposed to be a beneficial procedure for the prompt, cost effective and non-invasive diagnostic procedure of abdominal disease conditions in dogs.

CHAPTER ONE: INTRODUCTION, OBJECTIVES AND JUSTIFICATION

1.1 INTRODUCTION

The abdominal cavity of the domestic dog (*Canis lupus familiaris*) is the space contained in the trunk, partially covered by the rib cage dorsally, diaphragm cranially, muscle wall laterally and the pelvic cavity caudally. Abdominal organs are; the stomach, spleen, liver, gall bladder, kidneys, intestines, prostate, pancreas, adrenal glands, uterus, urinary bladder, mesentery, lymph nodes, blood vessels and nerves. These organs perform various metabolic, physiologic, endocrinologic and reproductive functions. Diagnosis of abdominal disease conditions is challenging due to the involvement of multiple organ systems and the diverse nature of clinical and pathological changes (Dyce *et al.*, 1996).

Some of the manifestations of abdominal disease conditions include vomiting, regurgitation, retching, ascites, palpable masses, diarrhoea, body wasting, melena, hematemesis, tenesmus, bloating and constipation. Diagnosis is based on history, clinical examination, and confirmatory tests such as haematology and clinical chemistry. In most cases, confirmatory diagnostic tests are required to confirm clinical diagnosis. These include abdominocentesis with fluid evaluation, exploratory laparotomy and post mortem examination (Tams, 2003).

Diagnostic imaging is a vital component of evidence based medicine. It allows the visualization of the internal structure of abdominal organs and interpretation of disease. Imaging also allows for non-invasive techniques to confirm diagnosis. The diagnostic imaging techniques available for small animal practice include radiography, ultrasonography, endoscopy, computed tomography, magnetic resonance imaging and scintigraphy. The extent of their use may be limited by availability, cost and expertise.

Despite global trends in diagnostic imaging, radiography remains the most commonly used technique in developing countries, including Kenya. The use of radiography as the sole imaging technique has limitations in the differentiation of soft tissue masses. The technique is also not sufficient in identifying masses surrounded by fluid. In such cases, ultrasonography is recommended to complement radiography (Freeman, 2002; Hayward, 2006).

Ultrasound enables detection of changes in organ size, shape, tissue density, internal structure and position of the organ. Abdominal organ ultrasound has greater accuracy, and provides greater diagnostic confidence compared to radiography (Sharma *et al.*, 2011). However, no studies have been reported on the use of ultrasonography in the diagnosis of abdominal disease conditions in dogs in Kenya.

The purpose of this study therefore was to establish a model framework for the diagnosis of abdominal disease conditions in dogs. The findings of the study were aimed at aiding in quick diagnosis and management of small animal patients presented with clinical signs of abdominal disease conditions.

1.2 OBJECTIVES

1.2.1 GENERAL OBJECTIVE

The general objective of the study was to enhance the use of ultrasound in the diagnosis of abdominal disease conditions in dogs.

1.2.2: SPECIFIC OBJECTIVES

The specific objectives of this study were to:

1. Relate the clinical features of abdominal disease conditions and ultrasound findings in dogs.
2. Compare the ultrasonographic appearance of abdominal organs in normal and diseased dogs.
3. Determine confirmatory diagnosis using ultrasound supported by other necessary tests.
4. Determine organ measurements by ultrasound in different age groups and breed type of normal dogs.

1.3 JUSTIFICATION

The University of Nairobi Small Animal Clinic (SAC, UON) serves as a referral centre in Nairobi and its environs. Due to the high cost of the ultrasound machine and difficulties in interpretation of the images, there are challenges in the use of ultrasound as an imaging technique. The value of using ultrasound with other supporting techniques in diagnosis of abdominal disease conditions in dogs has not been established at this clinic. The study was designed with the aim to address this gap by evaluating ultrasonography as a complement to other diagnostic tools such as; radiography, abdominocentesis, hematology, clinical chemistry, laparotomy and post mortem examination in diagnosis of abdominal disease conditions in dogs.

CHAPTER TWO: LITERATURE REVIEW

2.0 Introduction

Ultrasound is an easy to perform and non-invasive imaging modality (Lamb, 1990[1] Freeman, 2002) in diagnosing various diseases (WHO 1998; Hanazono *et al.*, 2013). Ultrasound is available in A (Amplitude) mode, B (Brightness) mode, M (motion) mode, Real time mode and Doppler. The development of B-mode, gray scale, real time scanning systems in the early 1980s catapulted diagnostic ultrasonography to the fore front of human medicine and thereafter veterinary medicine (Lattimer, 2000).

2.1 Ultrasound principles

The ultrasound machine utilizes high frequency sound waves to create an image. It does so via a transducer (probe) which produces the sound and receives reflected waves. There are two kinds of electronic probes available at the University of Nairobi Small Animal Clinic. The two kinds of types are based on the type of footprint; linear and convex. The linear array probe is usually long and has a rectangular footprint. The convex array probe is curved and has a convex footprint. The image produced by a convex probe is fan shaped while the image produced by a linear probe is rectangular shaped. The probe is lined with 64 piezoelectric (Quartz) crystals arranged in a straight line. Probes can further be classified as manual or electrical. Electrical probes have a fixed crystal platform, where the beam is produced. Mechanical probes have a motor which rotates the crystal platform.

The piezoelectric crystals are electronically sequentially excited in groups yielding either a rectangular or concave image depending on the probe type. When charged by a voltage, the crystals vibrate causing ultrasound waves (pulse) to be produced at a set frequency. Once the sound waves hit a tissue interface of different densities, some sound waves are reflected back (echo) and are detected by the piezoelectric crystals. These produce a corresponding current, which is converted to a two dimensional digital image on the machine monitor which depicts the tissue appearance (Lamb, 1995, Barr; 1988).

The appearance of tissues depends on the acoustic impedance. This is based on their density and velocity of the sound in the tissue (Burk and Feeny, 2003). The ultrasonographic appearance may be described as dark (anechoic/ no echoes), grey (hypoechoic / low intensity echoes) or white (hyperechoic / high intensity echoes). It may also be isoechoic (echotexture similar to some other adjacent structure or organ). Where an image has all the varying mixture of descriptions, it is referred to have heterogenous echogenicity (Lamb, 1995).

Abdominal organs show variation in size between breeds and also with age, gender and weight (Lamb, 1995). Ultrasound facilitates the measurement of tissues by use of the internal callipers. The size of organs is measured by callipers in the machine software which allow for a two dimensional measurement of the organ (Lamb, 1995). The ultrasound equipment can also be used to measure the area and estimate the volume occupied by these lesions.

2.2 Diagnostic uses of ultrasound

Ultrasonography is a primary diagnostic technique in several circumstances. These include; discriminating cystic verses solid masses; examining the body cavities filled with fluids that prohibit radiographic evaluation; discriminating the texture of suspected solid masses; locating non- radiopaque calculi within organs; cardiac evaluations; muscle and tendon evaluation; pregnancy diagnosis; and cystocentesis (Lamb, 1995; Lattimer, 2000). Other uses are collection of samples through ultrasound guided biopsies from lesions directly with reduced incidence of normal tissue damage.

Ultrasound allows visualization of internal structure of parenchymatous and luminal organs. The internal structure of luminal organs is established by the machines‘ ability to distinguish between the different layers of the luminal wall. The stomach and intestinal segments are assessed for wall layering, luminal contents, wall thickness, wall symmetry and motility (Agthe, 2009; Watson, 2010). The ultrasonographic appearance of the stomach layers may be described as follows; serosal surface- hyperechoic, muscularis layer- hypoechoic, submucosal layer- hyperechoic, mucosal layerhypoechoic and the lumen with gas and mucosal surface -hyperechoic (Tams, 2003: Agthe, 2009). The thickness of the wall in the dog has been established as 3-5 mm for the normal gastric wall, 3- 4.5mm for the normal intestinal wall and 2.5-3mm for the colon. This forms the basis for ultrasonographic diagnosis of gastroenteric disease manifesting atrophy or hypertrophy of the wall (Lamb, 1995).

Ultrasonographic diagnosis of lesions of the urinary bladder and uterus is based on assessment for wall layering, luminal contents, wall thickness and wall symmetry, for example in cases of cysts and tumors. Ultrasonographic delineation of the urinary bladder wall is best examined with a full bladder, which facilitates acoustic enhancement, hence giving clearer images. An example of this includes

ultrasonographic assessment of transitional cell carcinomas which is achieved on the basis of the extent of wall involvement; this also acts as a prognostic indicator (Hanazono *et al.*, 2013).

Previously, the uterus was primarily scanned for pregnancy diagnosis. However, ultrasound can also be used in the assessment of uterine pathologies such as pyometra and endometrial hyperplasia (Lattimer, 2000).

The dimensions of the liver cannot be adequately established due to the overlapping liver lobes. However, the area at which the liver can be imaged has been established as the right abdominal flank caudal to the ribs (Tams, 2003). The spleen is located on the left side, caudal to the last rib.

Other organs which can be examined in the dog using ultrasound include; lymph nodes (Agthe, 2009) and adrenal gland (Choi *et al.,* 2011; Lamb, 1990_2). In addition, advances in ultrasound facilitate the use of Doppler ultrasound of the abdomen for the assessment of flow in blood vessels (Boswood and Lamb, 2005; Lamb, 2005).

Ultrasound has also been used to detect free abdominal fluid in patients following road traffic accidents (RTA) due to blunt force trauma. The procedure is non-invasive and takes an average of 3 minutes. This laid the platform for management based on their abdominal fluid score (AFS) using an abdominal focused assessment with sonography for trauma (AFAST) protocol (Lisciandro, 2011).

2.3 Image interpretation and artefacts

The interpretation of ultrasonographic images requires the sonographer to possess knowledge on the anatomy of the area. Ultrasound allows for examination in horizontal and vertical views. Image interpretation is based on changes in size, shape and echotexture (Cartee, 1995). Understanding the normal anatomic location of the organ of

interest also determines selection of the acoustic window in order to achieve the best image quality. It also helps in the selection of the type and frequency of ultrasound probe to be used for diagnostic ultrasound. Selection of the probe type depends on the anatomic location of the organ of interest, with specialized probes designed with varied footprint sizes to avoid interference with bone structures. Most probes have multiple frequencies which can be varied depending on the depth of the organ of interest. Organs located deeper beneath the skin are scanned using lower frequencies, while superficial organs are scanned using higher frequencies (Lamb, 1995).

An artifact is defined by the International Dictionary of Medicine and Biology as ―any *record or image obtained in the course of applying a medical diagnostic technique which is not representative of the structures under study but is adventitious*‖. During the evaluation of anatomic structures, acoustic artefacts result in added, missing, improperly located, brightness, shape or size alterations (Kirberger, 1995).

Knowledge of the artefacts which can be encountered during imaging is important for accurate interpretation. Artefacts are classified based on their aetiology as operational artefacts and environmental artefacts. Environmental artefacts are as a result of interference with the environment. These include electromagnetic interference (e.m.f) from clippers, radio-frequency signals or fluorescent lighting (Kirberger, 1995).

Operational artefacts are due to operator causes. These include: interference from air trapped in hair or luminal organs, improper transducer selection and improper gain settings. Due to the nature of the causes of these artefacts, an understanding of the physics of ultrasound is vital (Kirberger, 1995).

It is important to note that some artefacts are useful as they help assess the nature and structure of images visualized. Examples of such useful artefacts include: acoustic shadows; acoustic refractions and reflection; acoustic enhancement and propagation

speed errors. Acoustic shadows are useful in that they vary depending on the cause. These therefore give the sonographer the etiology of the shadow e.g. clear shadows are seen when mineralized compounds such as bone or calculi are the cause the shadows. Examples of acoustic refraction and reflection artefacts are: reverberations, ring down, edge shadows and comet tails (Kirberger, 1995).

Some artefacts are termed as confusing and are associated with pulse and beam characteristics. These include: mirror images; multipath, ghost and split image artefacts, slice thickness artifact/ section thickness/ beam thickness/ beam averaging/ partial volume effect thickness and range ambiguity artefacts. Most of these artefacts can be overcome by the awareness that they are a possible event and compensatory movement or placement of the probe to overcome the possibility. In addition, proper patient preparation e.g. shaving and patient placement contribute to elimination of these errors (Kirberger, 1995).

2.4 Advances in the use of ultrasound technology

Ultrasound has evolved from its conventional diagnostic use to the non-conventional such as Doppler. This facilitates the evaluation of tissue perfusion, which is reduced in thrombi obstruction and increased in tumors (Lattimer, 2000).

Ultrasound is also used in the ante mortem and post-mortem grading of carcasses. Examples of these include; back fat thickness in pigs and muscle cover in turkeys are determined using specially designed transducer probes. Ultrasound is used also to determine the sex of fish in aquaculture and foetuses in domestic and wild animals.

The development of transducer probes to conform to various shapes and sizes has allowed the integration of ultrasound technology into fields not previously considered. Probe sizes are modified to fit into scanning windows for more accurate scanning of

specific organs. This overcomes the limitations caused by gas filled viscous organs and mineralized tissues. For example, oesophageal probes allow scanning of the heart without the interference of the gas in the lung tissues which causes acoustic shadows (Burk and Feeney, 2003).

In addition, ultrasound contrast media using gas microbubbles is used in determination of perfusion parameters of disease solid mass tissues such as tumors. This media acts as an eco-enhancer to the beam allowing for better visualization of tissue perfusion.

Animals with tough exoskeletons such as turtles and tortoises can benefit from ultrasound due to specially designed probes which facilitate scanning. In turtles, biconvex sector scanners are used due to their small footprints as a result of smaller acoustic windows in these species.

With further developments in the imaging field, ultrasound has become a more routine clinical examination procedure that facilitates early detection of pathology with minimum costs and minimum risk of tissue damage (Lattimer, 2000).

CHAPTER THREE: MATERIALS AND METHODS

3.0 Study design

The study was designed as purposive. This was based on the fact that the University of Nairobi Small Animal Clinic serves as a referral clinic for several other privately owned clinics in Nairobi area. Therefore, it had a sampling population representative of the dogs in Nairobi and its environs.

3.1 Study animals

The criteria for inclusion was that; dogs presented with any of the clinical signs indicative of abdominal disease conditions; vomiting, retching, diarrhoea, ascites, a palpable mass, wasting, icterus, tenesmus, constipation, hematemesis, urinary incontinence, hematuria, stranguria, discharges from the vulva and melena. Twenty five dogs met the selection criteria and were therefore recruited into the study group as seen in Table 3.1 below.

Table 3.1: Selection criteria of the 25 study animals.

CASE	BREED	AGE	CLINICAL SIGNS
1	2	C	Gradually enlarging abdomen
2	2	B	Hematuria
3	2	C	Enlarged abdomen, anorexia
4	2	C	Enlarged abdomen
5	2	C	Enlarged abdomen
6	2	B	Vomiting, enlarged abdomen
7	2	C	Enlarged abdomen
8	2	B	Enlarged abdomen
9	2	C	Anorexia
10	1	B	Chronic diarrhoea
11	2	B	Enlarged abdomen, vulval discharge
12	1	B	Hematuria, urinary incontinence
13	1	C	Urinary incontinence
14	2	B	Enlarged abdomen, emaciation
15	2	C	Hematuria, emaciation
16	2	B	Palpable masses on the ventral abdomen
17	1	B	Palpable ventral swelling
18	2	C	Abdominal enlargement
19	2	C	Abdominal pain, anorexia, diarrhoea
20	2	C	Obstipation, enlarged abdomen
21	2	B	Abdominal straining with vulval discharge
22	2	B	Gradually enlarging abdomen
23	2	B	Difficulty in parturition with vulval discharges

24	2	D	Ventral swelling on the skin around the mammary gland
25	2	B	Vulval discharge

Key: 1: Small breed dogs, 2: Large breed dogs; B: >1year to < 5 years, C :> 5years to <10 years D: >10 years.

In addition, thirty normal dogs were purposively selected for ultrasonographic examination. The general condition, clinical examination and complete blood count (CBC) were evaluated and found to be within normal range.

For the two groups, dogs selected were then divided further into groups based on age and breed type. Large breed dogs included all study dogs weighing more than 25kgs, with large body frames or any of the following breeds: German shepherd, Rotweiller, Doberman pinchers and their crosses. Small breed dogs included all study dogs weighing less than 25kgs, with small body frames or any of the following breeds: Japanese Spitz, Terriers, Maltese and their crosses. This criterion for grouping by breed type was based on past records of the most commonly presented dogs at the Small Animal Clinic. Large breeds were termed as group 1 while small breeds were termed as group 2.

Grouping of dogs by age was based on dentition, the extent of wear and tear and owners‘ history when available. Dogs were assigned into 4 groups as follows: group A: 0≤1year; group B: >1<5 years; group C: ≥5<10 years and group D: ≥ 10 years. This criterion for grouping by age was based on past records of dogs presented to the Small Animal Clinic.

3.2 Scanning procedure

The dogs were prepared for scanning by shaving the ventral abdominal region starting from the area around the xiphoid cartilage up-to the inguinal region. On the lateral aspects, shaving included the area caudal to the 8^{th} intercostal space, extending caudally up-to the coxo-femoral joint. Where the client did not give consent for shaving of the dog, the hair was made wet using ethyl alcohol prior to scanning and a latex cover used to protect the probe. A coupling gel was then applied on the body surface or probe.

The ultrasonographic examinations were performed using a variable 3.5 to 6.5 MHz convex transducer (Figure 3.1) with a Kontron digital ultrasound machine (Model Sonia VET, Germany®) (Figure 3.2).

Figure 3. 1: Photograph of a convex array probe of the machine used in the study. A-footprint.

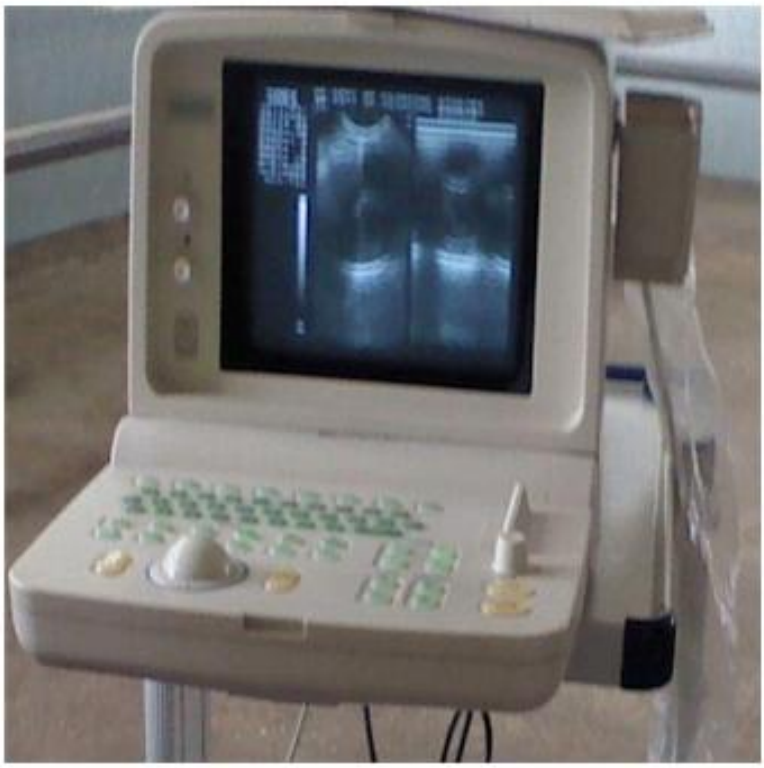

Figure 3. 2: Photograph of the ultrasound monitor with control panel in use.

Dogs which were not cooperative to handle were sedated using Xylazine Hydrochloride (Bomazine®20g/ml) at a dosage of 1.1mg per kilogram body weight administered intramuscularly. Cooperative dogs were manually restrained after being muzzled for operator safety. The dogs were then positioned in either left lateral or right lateral recumbency to facilitate scanning of the organ of interest. The liver, spleen, left and right kidneys, stomach, intestines, urinary bladder and uterus were scanned depending on the most important clinical indication of disease. The images of the organs were printed and electronically archived.

Organs were measured using the internal callipers of the scanner for wall thickness, vertical and horizontal dimensions where applicable. The organs measured included; the kidney for horizontal and vertical kidney diameter. The wall thickness for the stomach, intestine and urinary bladder were taken and in addition their contents were examined. These measurements were stored onto a Microsoft excel spread sheet.

3.3 Clinical Examination

All the dogs selected for the study (twenty five) and control group (thirty) were screened by physical examination for diseases.

3.3.1 Confirmatory tests

Study animals were subjected to one or more of the following confirmatory tests; radiography, haematology and clinical chemistry, abdominal fluid analysis, exploratory laparotomy, histo-pathological and post mortem examinations. This was based on the diagnosis, prognosis, clinical indications, availability and costs of additional tests.

3.3.1.1 Blood smear evaluation

Blood was evaluated by use of a blood smear which was prepared for a differential white cell count and general morphological features of the red blood cells. A drop of blood was collected from the tip of the ear and put on a glass slide. The blood was allowed to air dry. The blood smear was fixed using Methanol 95% for 5 minutes and removed thereafter and allowed to air dry. It was subsequently stained using Giemsa stain, diluted 1 into 5 (20%) for 15 minutes and thereafter air-dried. The blood smear was viewed under a magnification of □100 using oil immersion lens of a light microscope (Lattimer *et al.*, 2003).

For this study blood smears served as a basic screening technique for the entire control group. This was due to the fact that the test is easy to do, inexpensive, widely used and available to all clinicians. Two samples from animals in the study group were evaluated using this test.

3.3.1.2 Radiography

Radiography was carried out using a Philips Practix 33 Plus machine®. Orthogonal radiographic views were taken of the organ of interest. This was done by placing the patient on a buckey table. Patients that were difficult to handle were sedated using Xylazine Hydrochloride (Bomazine®20mg/ml) at a dosage of 1.1mg per kilogram body weight administered intramuscularly to facilitate positioning of the patient and personel safety during radiography. The patients were exposed to KVs commensurate to the required view to be taken. Eleven study animals were tested using this confirmatory test.

3.3.1.3 Clinical chemistry

Blood was collected from the cephalic vein of each animal and allowed to clot in plain vacutainers. Serum was separated using a table centrifuge and stored in ependorff tubes. A kinetic photometric test kit, (according to the International Federation of Clinical Chemistry and Laboratory medicine (IFCC)) was used. A spectrophotometer (The Visual® Biomerieux) was used together with a kit manufactured by DiaSys Diagostic systems, Germany. Liver function tests performed included; Alanine aminotransferase (ALT) and Alkaline phosphatase (ALP) (Lattimer *et al.*, 2003).

Kidney function tests performed included blood urea nitrogen (BUN) and Creatinine. Other tests of interest were serum albumin and total plasma protein concentration. Five serum samples were tested using this method, due to limitations of costs of tests to clients.

3.3.1.4 Urinalysis

Urine was collected via either urinary bladder catheterization or transcutaneous cystocentesis. The sample was stored into universal bottles and immediately analysed using 10 SGL strip dip sticks (Uriscan YD Diagnostics®, Germany). The dipstick was dipped into the sample up to the graduated mark and read after 60 seconds. Clinical values measured using this technique included; blood, bilirubin, urobilinogen, ketones, protein, nitrite, glucose, pH, specific gravity and leucocytes. The results where then compared to the published normal clinical chemistry values for dogs. Three urine fluid samples were tested using this method.

The urine sample was put into an ependorff tube and placed into a low speed centrifuge. This was centrifuged at 1500 revolutions for 5 minutes. The supernatant was removed and sediment suspended in the remaining volume of urine. The drop of sample was placed on a microscope slide; a coverslip applied and examined unstained using a light microscope X40 objective. The sample was examined for RBC, epithelialelial cells, leucocytes, casts, crystals, bacteria and yeast cells (Lattimer *et al*, 2003).

3.3.1.5 Fluid analysis

Fluid was collected via aseptic para-centesis. The sample was stored into universal bottles and immediately analysed using 10 SGL strip dip sticks (Uriscan YD Diagnostics®, Germany). The dipstick was dipped into the sample up to the graduated mark and read after 60 seconds (Lattimer *et al*, 2003).

Clinical values measured using this technique included; blood, bilirubin, urobilinogen, ketones, protein, nitrite, glucose, pH, specific gravity and leucocytes. The results were then compared to the published normal clinical chemistry (Merck Veterinary manual) values for dogs. One fluid sample was tested using this method.

3.3.1.6 Exploratory laparotomy

Exploratory laparotomy was performed for nine cases that was to undergo emergency surgical procedures and with consent from the owner. Preparation for aseptic surgery entailed shaving the area around the proposed incision line, scrubbing and draping. General anaesthesia was achieved using Xylazine Hydrochloride (Bomazine® 20mg/ml) at a dose rate of 1.3mg per kilogram body weight. After 10 minutes, Ketamine Hydrochloride (Ketamax ®50mg/ml) at a dose rate of 10mg per kilogram body weight was administered intramuscularly. Top up rations were administered as a cocktail of the two drugs at half the dosage. A ventro-midline incision was made extending from the umbilicus to the inguinal area. The organ of interest was visualized and observations noted. Nine animals were subjected to exploratory laparotomy to confirm diagnoses.

3.3.1.7 Post mortem examination

Nine study animals with poor prognosis, and those whose owners gave consent, were humanely euthanized using rapid intravenous Sodium pentobarbitone (200 mg/ml Eutha-naze ®,Bayer Health Care South Africa) at a dose rate of 200mg per kilogram body mass. Routine post mortem examination was performed. The organs of interest were further visually examined and photographed. Tissues were collected and routinely fixed in 10% formalin solution for 10days and routinely processed for histopathological examination.

3.3.1.8 Histological processing

The sampled tissues were sized to 10 cubic mm in volume. They were fixed in 10% buffered formalin for 48 hours. Once fixed, the tissues were trimmed to a thickness of 2mm and a size small enough to fit on a glass slide. The trimmed tissues were then processed, undergoing the process of dehydration in increasing concentrations of alcohol (Ethanol), cleared using Amyl acetate and Xylene, and infiltrated using molten

embedding wax. Once infiltrated, the tissues were embedded in embedding wax, separated, sectioned, and placed onto clean glass slides coated with an adhesive (egg albumin). These slides were left in a dry air oven at 45 degrees centigrade to melt away wax residues.

For staining, the sections already adhered to glass slides were allowed to cool to room temperature. They were then placed in Xylene to clear any remaining wax residue, rehydrated in decreasing concentrations of alcohol and distilled water, stained with Hematoxylin for 10 minutes, washed in a gentle stream of water for 10 minute, stained with Eosin for 5 minutes, washed in a gentle stream of water for a 10 seconds, dehydrating in increasing concentrations of alcohol for a 10 seconds, cleared for alcohol using xylene and then mounted with a coverslip using DPX mountant. The mountant was allowed to dry for a 3 hours before microscopic examination (Lattimer *et al.*, 2003).

Five cases were confirmed using this technique. The photomicrographs displaying histopathologic features are presented under corresponding organ sections.

3.4 Data analysis

Data collected was entered into Microsoft Excel software and categorized according to breed type and ages. The organ images were analysed to compare the mean size differences between the age groups (A, B, C and D), Figure 3:1, and thereafter between the different breed types (Small and Large). Data from study animals was also analysed to compare the means with the control group. However, only the measurements of organs with pathology in the study group were analysed.

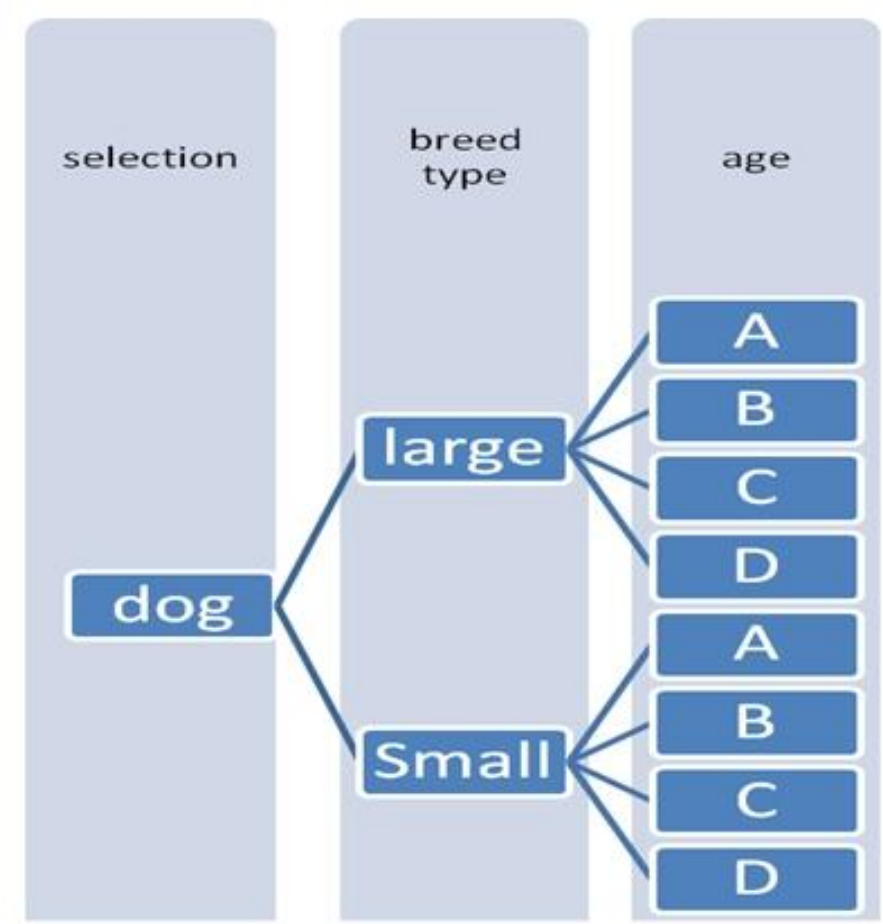

Figure 3. 3: Patient selection (Key: Small breed dogs, Large: Large breed dogs, A :> 0<1year, B :> 1year to<5 years, C :> 5years to <10 years D: >10 years).

CHAPTER FOUR: RESULTS

4.0 Study results

The results of the examination of abdominal disease conditions are classified and presented according to the organs they affected. This chapter outlines the anatomic location echotexture, sonographic and results of the confirmatory tests. The organs discussed included; liver, intestine, stomach, urinary bladder, uterus, kidney and spleen with their respective conditions. It is important to note that the normal ultrasonographic findings of organs are described based on the control group and in reference to what other authors have described.

The pathologic findings of each organ evaluated are described in the text and illustrated by the sonograms or photographs where applicable. A summary of the cases in the study group is presented in Table 3.1 below.

Table 4. 1: Study case summary. Key1: Small breed dogs, 2: Large breed dogs; B: >1year to<5 years, C :> 5years to<10 years D: >10 years.

Case	Breed	Age	Clinical signs	Ultrasonographic features	Confirmed diagnosis
1	2	C	Gradually enlarging abdomen	Ascites	Liver cirrhosis
2	2	B	Hematuria	Bladder calculi	cystourolithiasis
3	2	C	Enlarged abdomen, anorexia	Cholangiohepatitis	cholangiohepatitis
4	2	C	Enlarged abdomen	Splenic mass	hemangiosarcoma
5	2	C	Enlarged abdomen	Splenic mass	hemangiosarcoma
6	2	B	Vomiting, enlarged	distended uterus	pyometra

			abdomen		
7	2	C	Enlarged abdomen	Rounded liver lobes	Liver cirrhosis
8	2	B	Enlarged abdomen	Foetal parts	pregnancy
9	2	C	Anorexia	Rounded liver mass	Liver cyst
10	1	B	Chronic diarrhoea	No significant findings	
11	2	B	Enlarged abdomen, vulval discharge	Distended uterus	pyometra
12	1	B	Hematuria, urinary incontinence	Bladder calculi	cystourolithiasis
13	1	C	Urinary incontinence	Bladder crystals	cystoliths
14	2	B	Enlarged abdomen, emaciation	Rounded liver lobes	Liver cirrhosis
15	2	C	Hematuria, emaciation	Bladder mass	Transitional cell carcinoma
16	2	B	Palpable masses on the ventral abdomen	Intestinal segments	Ventral hernia with intestinal contents and tear of abdominal muscles
17	1	B	Palpable ventral swelling	Intestinal segments	Ventral hernia with intestinal contents
18	2	C	Abdominal enlargement	Enlarged renal pelvis	Hydronephrosis
19	2	C	Abdominal pain,	No significant	peritonitis

			anorexia, diarrhoea	findings	
20	2	C	Obstipation, enlarged abdomen	No intestinal movement	Paralytic ileus
21	2	B	Abdominal straining with vulval discharge	Foetal parts with foetal heartbeats	Dystocia with viable foetuses
22	2	B	Gradually enlarging abdomen	Foetal parts	pregnancy
23	2	B	Difficulty in parturition with vulval discharges	Foetal parts with no foetal heartbeats	Dystocia with stillborn pups
24	2	D	Ventral swelling on the skin around the mammary gland	Irregular mass in the subcutaneous tissue	Mammary gland tumor
25	2	B	Vulval discharge	Distended uterus	pyometra

4.1 The liver

4.1.1 Anatomic location

The liver is located caudal to the diaphragm; it extends dorsally over the diaphragmatic hilus as shown in the Figure 4.1. It can be scanned by placing the transducer probe over the area caudal to the xiphisternum and the probe oriented cranially to view the longitudinal orientation of the liver. The probe is then moved laterally to the left and right para-lumbar fossa caudal to the costal arch. The gall bladder can be viewed at a space located on the right para-median, caudal to the xiphisternum. The gall bladder of the canine is normally ovoid in shape.

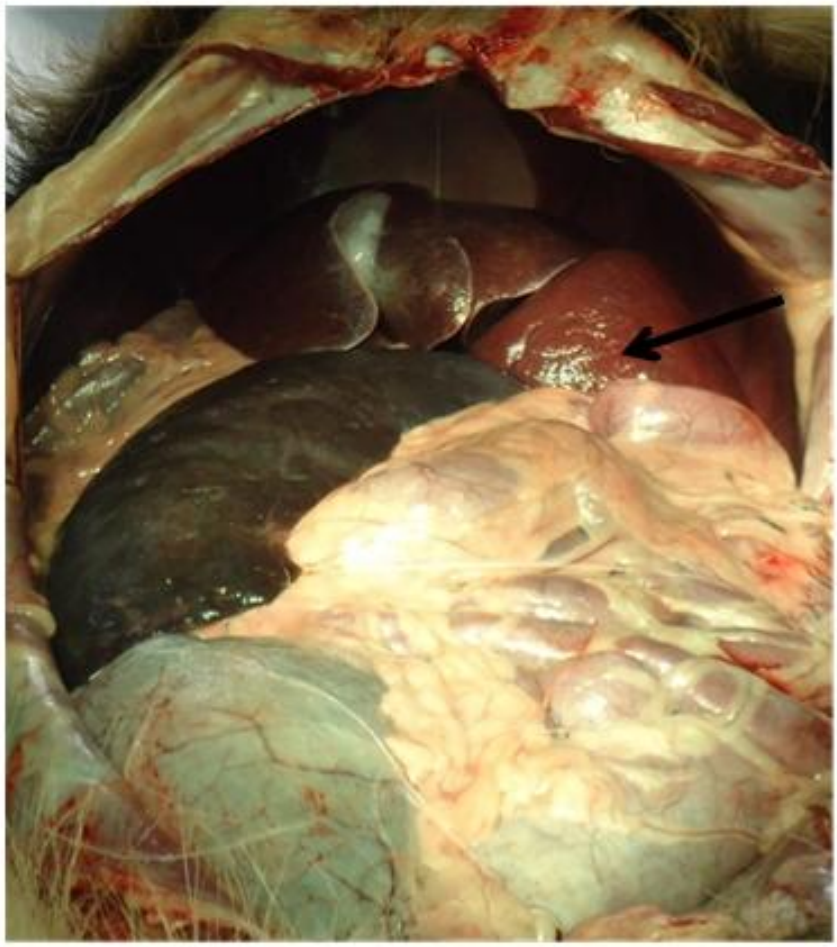

Figure 4. 1: Photograph of the approximate position of the liver indicated by a black arrow as seen following an exploratory laparotomy.

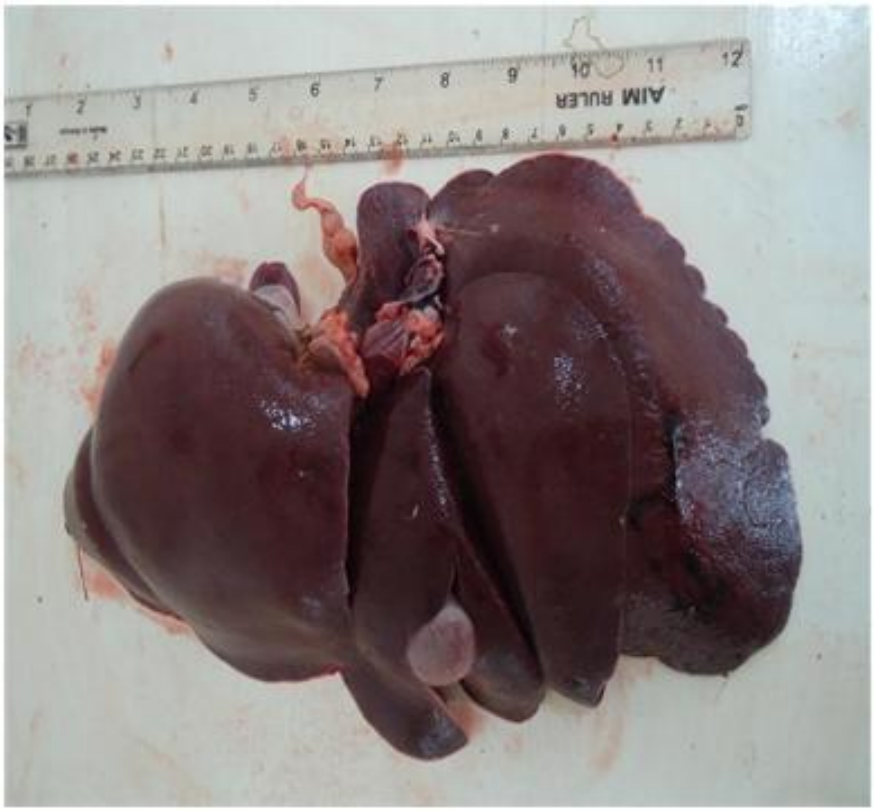

Figure 4. 2: Photograph of the normal liver appearance as seen following a post mortem of a euthanized animal.

4.1.2 Normal echotexture

Figure 4.3 shows portal veins which appear as anechoic in the lumen surrounded by a hyperechoic white border. The bile duct is also seen as an anechoic lumen with hyperechoic walls. The liver parenchyma appears as homogenously hypoechoic with focal zones of hyperechogenicity due to the vasothelium of the portal vessels.

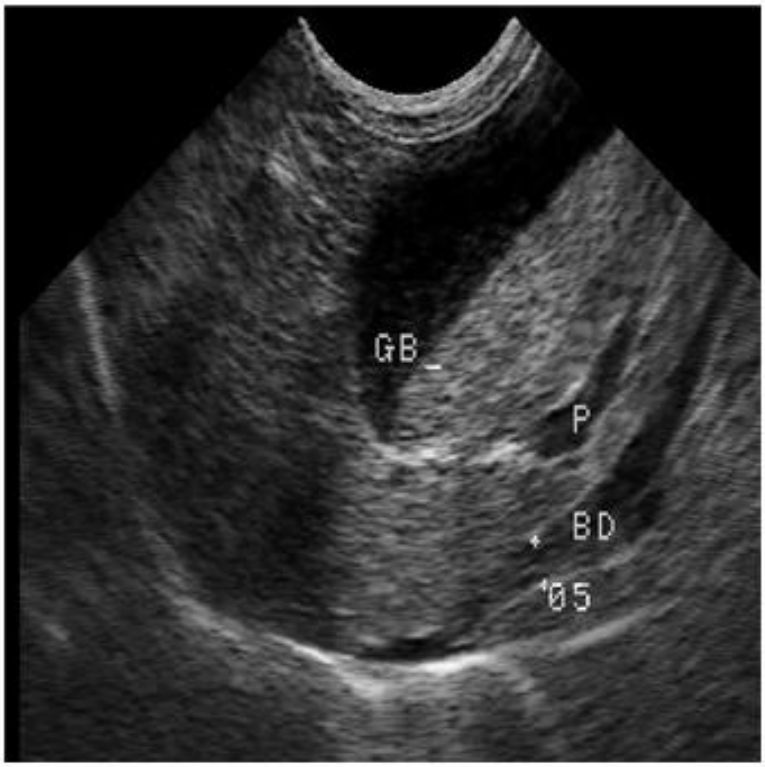

Figure 4. 3: Normal Liver sonogram GB-gall bladder, BD-bile duct; P-portal vessel; 0.5 the dimension of the bile duct.

4.1.3 Liver sonographic results

Five liver cases were reported in this study. This represented 20% of the pathological cases. Three cases were liver cirrhosis, one case of cholangiohepatitis and a one of a liver cyst.

Figure 4.4 shows a highlighted hyperechoic liver region in the distal portion of the image, which has obscured the gall bladder, indicative of cholangiohepatitis.

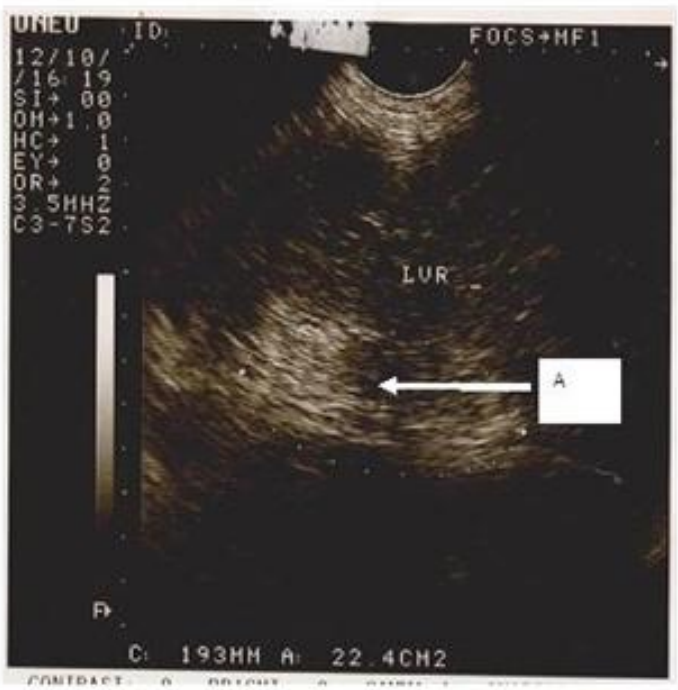

Figure 4. 4: Case 3 diseased liver sonogram-cholangiohepatitis. An arrow showing area of increased echogenicity in the liver parenchyma, LVR- normal liver parenchyma.

Figure 4.5 shows a sonogram depicting accumulation of fluid in the peritoneal cavity of a dog diagnosed with liver disease. The liver appears hyperechoic due to cirrhosis. Accumulation of fluid in the abdominal cavity delineates margins of the liver lobe appearing hyperechoic.

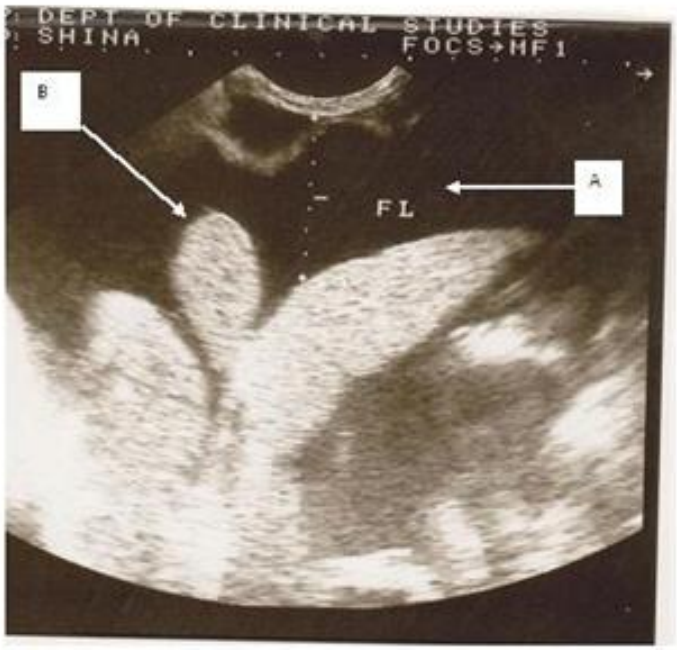

Figure 4. 5: Case 1 Diseased liver sonogram (liver cirrhosis). A- Rounded liver lobes. B- Anechoic fluid surrounding the liver, FL- fluid.

Figure 4.6 shows a large rounded well defined dark mass (anechoic) which was diagnosed as a liver cyst on exploratory laparotomy. Note the other dark rounded small mass which is the gall bladder.

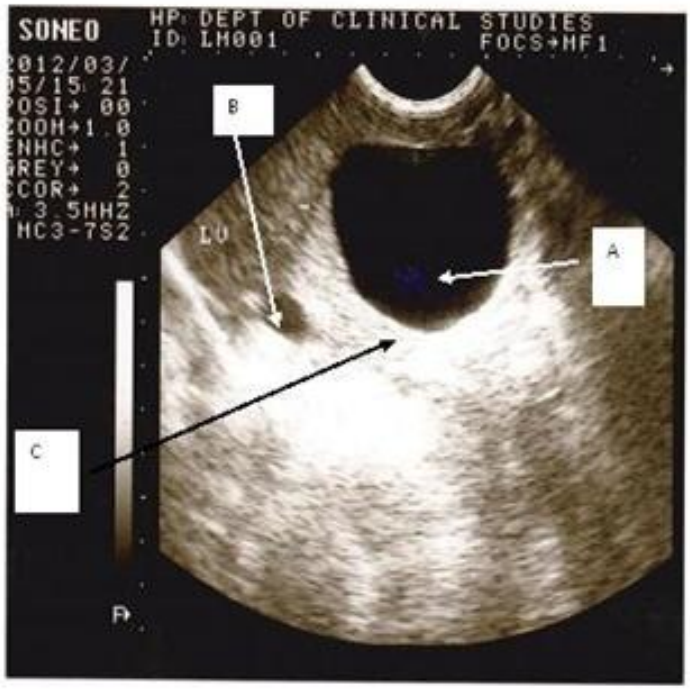

Figure 4. 6: Case 9 diseased liver sonogram. A is a liver cyst with anechoic fluid filled centre. B- Gall bladder. C increased echogenicity on the distal border due to acoustic enhancement.

4.1.4 Confirmatory tests for liver disease in dogs

Liver disease was initially diagnosed based on the clinical signs; i.e. abdominal enlargement with a pendulous appearance. Ballottement of the abdomen revealed presence of fluid. Jaundice was only reported in one case which had the most severe cirrhosis. Wasting was also seen in all the cases which exhibited liver disease.

Confirmation of the diagnosis was based on results from clinical chemistry (ALT and ALP), albumin and albumin-globulin ratio and the ultrasonographic changes. Table 4.2 presents results of the laboratory tests carried out to determine the liver function.

Table 4. 2 Liver function tests

Tests	**Normal Values IU/L**	**Results IU/L**
ALP	**(10-150)**	137(case 1)
		91 **(** case 3)
ALT	**(5-60)**	13 (case 1)
		22 (case 3)
Albumin	**(2.6-4.3) mg/dl**	1.5 **mg/dl** (case 1)
Albumin-globulin ratio	**(0.75-1.9)**	0.4 (case 1)

Relative size and colour changes of the liver were indicative of diseases as is seen in Figure 4.7 which shows the appearance of the liver when affected by cirrhosis as observed at post mortem examination.

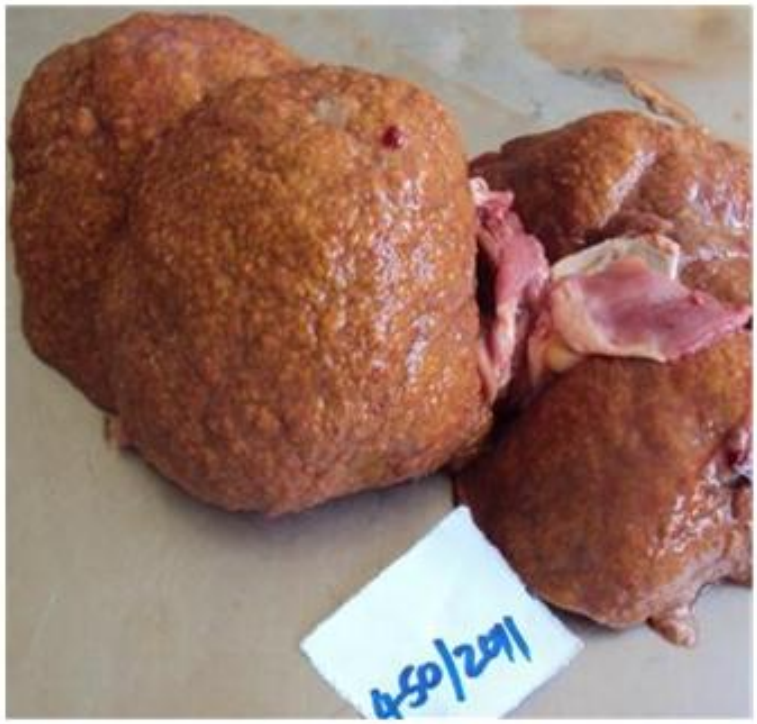

Figure 4. 7: Post mortem picture of liver case 1 with liver cirrhosis: the granular appearance of the liver surface and rounded edges were observed.

Histopathology of the liver samples which exhibited gross pathology of liver cirrhosis is described in the Figures 4.8, 4.9 and 4.10 below.

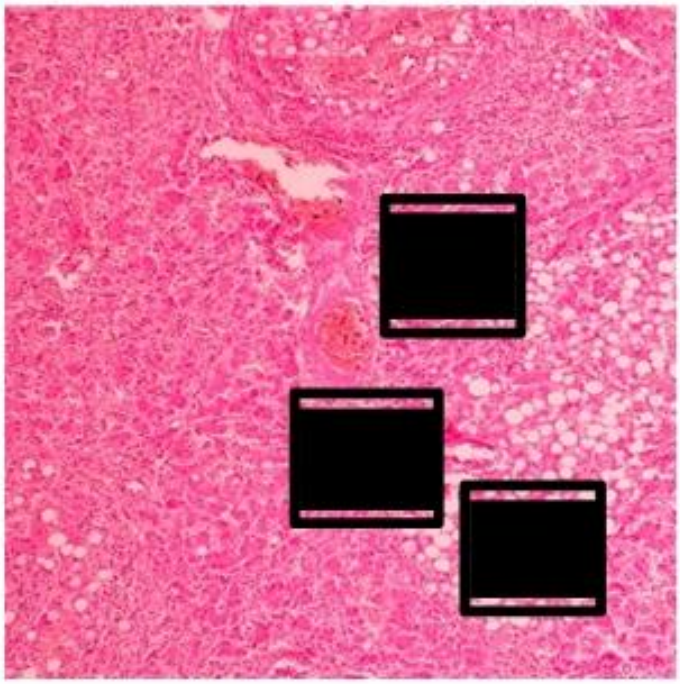

Figure 4. 8: Case 1 Photomicrograph of a liver section with liver cirrhosis with inserts [Hematoxylin and Eosin, 100x].

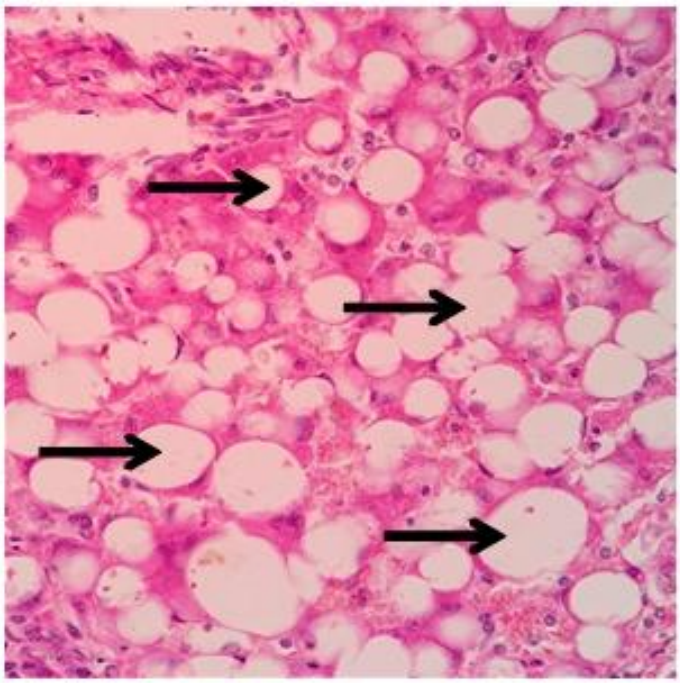

Figure 4. 9: Photomicrograph of a liver section with liver cirrhosis showing fatty degeneration of hepatocytes (black arrows) corresponding to Insert A in Figure 4.8 [Hematoxylin and Eosin, 400x].

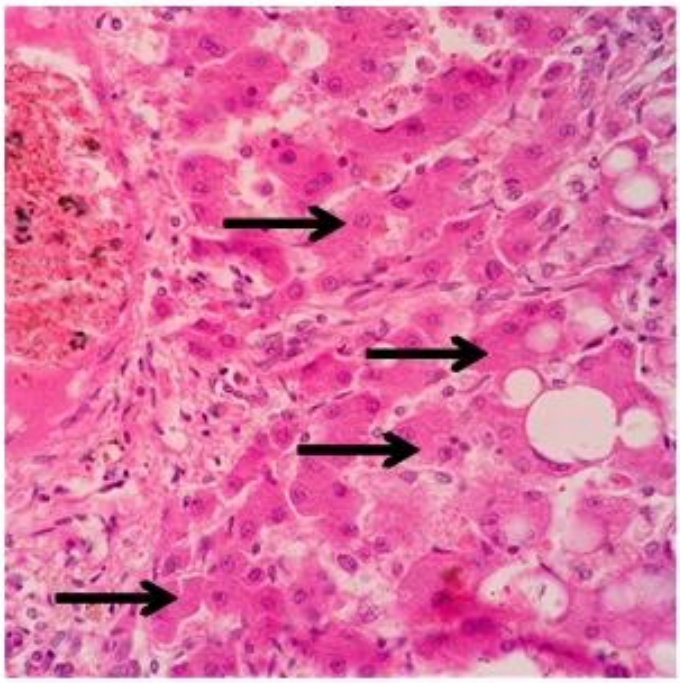

Figure 4. 10: Photomicrograph of a liver section with liver cirrhosis showing compensatory hypertrophy of hepatocytes (black arrows) corresponding to Insert B in Figure 4.8 [Hematoxylin and Eosin, 400x].

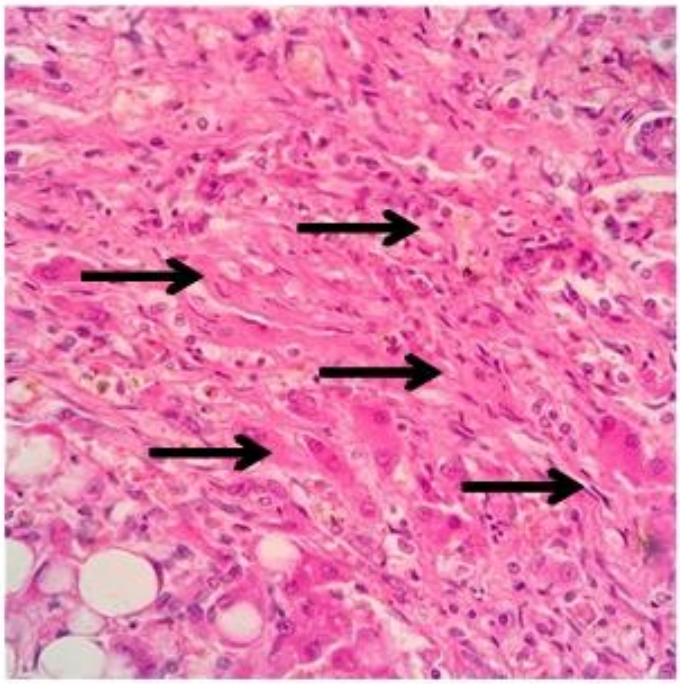

Figure 4. 11: Photomicrograph of a liver section with liver cirrhosis showing fibroplasia replacing degenerated hepatocytes (black arrows) corresponding to Insert C in Figure 4.8 [Hematoxylin and Eosin, 400x].

4.2 The kidney

4.2.1 Normal anatomic location

The normal canine kidney is ovoid shaped with well-defined borders. The renal architecture is divided into the renal cortex, medulla and pelvis. The right kidney is located caudal to the liver, in a recess on the caudal lobe as shown shaded in Figure 4.12. The left kidney is located at the left intercostal spaces of the 11^{th}, 12^{th} and 13^{th} rib. The kidneys can be visualized by scanning the space caudal to the 13^{th} rib on the right side and cranial to the 13^{th} rib on the left side (Lamb, 1995; Cartee, 1995).

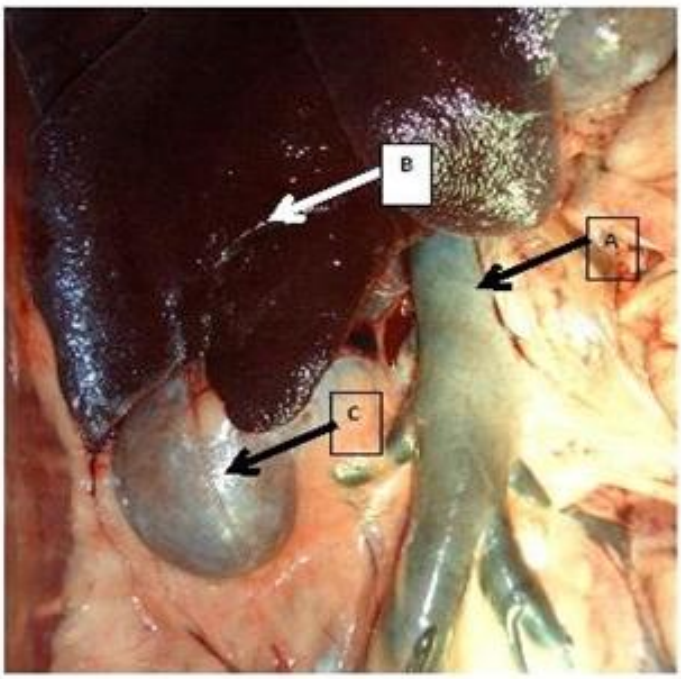

Figure 4. 12: Photograph of the kidney position in a normal dog obtained following exploratory laparotomy. A- abdominal aorta, B-liver and C-right kidney.

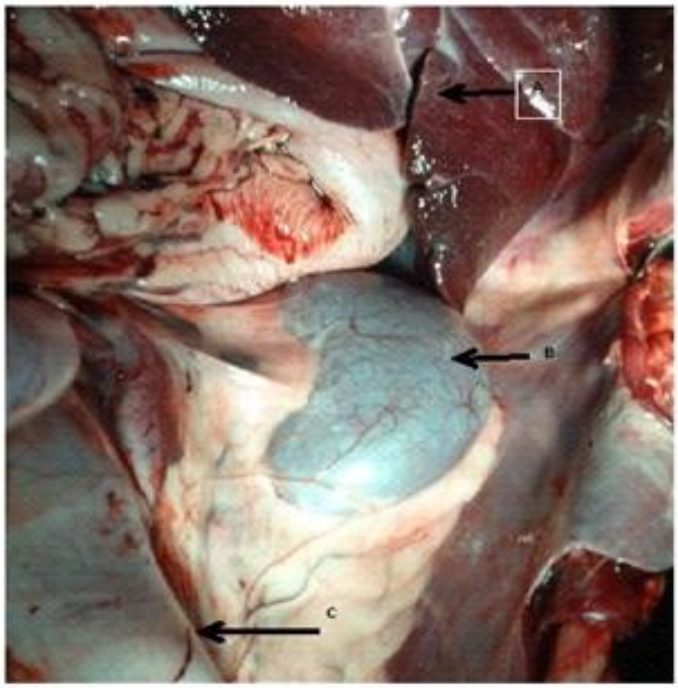

Figure 4. 13: Photograph of the kidney position in a normal dog obtained following exploratory laparotomy. A- liver, B-left kidney and C-rectum.

4.2.2 Normal echotexture

The renal cortex is slightly more hyperechoic than the renal medulla. The pelvis is hyperechoic with anechoic centre due to urine accumulation. The outline of the kidney is well defined due to fat and fibrous tissue.

4.2.3 Kidney sonographic results

In this study, only one case of kidney disease was reported out of twenty five cases presented. This represented 4% of the cases reported. A diagnosis of hydronephrosis was made whose aetiology was undetermined.

Figure 4.14 shows a sonogram of a kidney which appears darker due to accumulation of urine in the renal pelvis. The enlargement of the kidney was determined to be due to impaired urine flow as a result of blockade of the ureter.

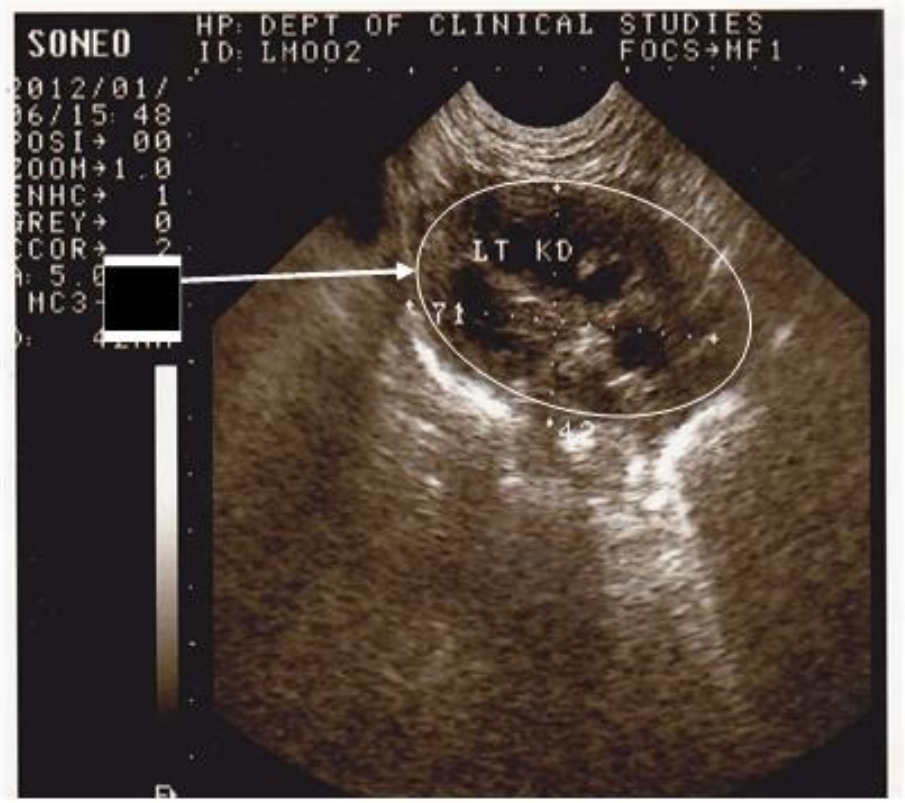

Figure 4. 14: Case 18; sonogram of the left kidney of a dog diagnosed with hydronephrosis, A- kidney outline. Note the anechoic pockets within the kidney which represent the renal medulla. Dimensions show a horizontal diameter of 7.1 cm by a vertical diameter of 4.2cm.

4.2.4 Confirmatory kidney function tests

The patient presented with an enlarged abdomen and urinary incontinence. The abdominal enlargement though not characteristic with kidney disease was attributed to urine retention in the urinary bladder.

Kidney function tests carried out included BUN and creatinine whose results are shown in Table 4.3.

Table 4. 3 Kidney function test results (case 18).

Test	**Normal Value mg/dl**	**results mg/dl**
BUN	**(7-27)**	256.8
Creatinine	**(0.4-1.8)**	5

From the results it was evident that there was functional damage to the kidneys evidenced by the increased concentrations of BUN and Creatinine.

4.3 The uterus

4.3.1 Anatomic location

The canine non gravid uterus is located dorsal to the urinary bladder, and at the region of the ventro-midline. The ovarian pedicles are oriented to their respective sides. The gravid canine uterus is displaced ventrally depending on the duration of pregnancy and the concurrent weight of each horn.

4.3.2 Echotexture of the uterus both gravid and non gravid

The normal uterus is not visible on ultrasound. The gravid uterus can be scanned on the ventro-midline caudal to the umbilicus. The gravid horns will have an echogenic wall due to acoustic enhancement by the fluid in the allantoic and amniotic sacs of the foetuses as seen in Figure 4.15. The foetal skeleton can be visualized as hyperechoic outlines. The endometrium is hypertrophied during pregnancy and will appear as hypoechoic. In addition the viability of foetuses can be determined as foetal movements with heart beats visible on the scanner.

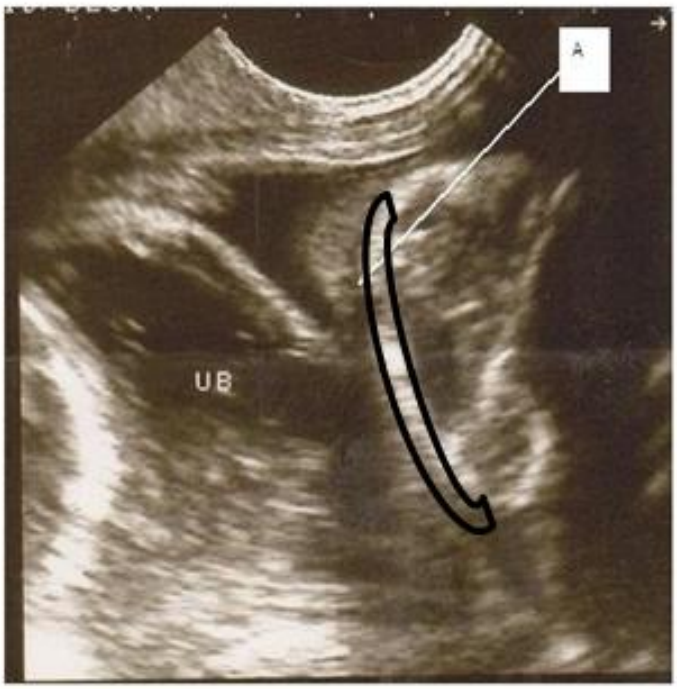

Figure 4. 15: Uterine sonogram with foetal parts-A; note the hyperechoic outline of the foetal bones. (Normal pregnancy) UB-uterine body.

4.3.3 Uterus pathology sonographic findings

Ultrasonographic examination revealed that seven out of twenty five dogs had uterine conditions. Of these, three were reported as having pyometra and four had physiological conditions i.e. pregnancy. Pregnancy was identified to be a finding in this study for purposes of description of uterine contents.

Figure 4.16 shows the uterus appearing anechoic to hypoechoic due to pus accumulation. The margins of the uterine wall appear well delineated due to acoustic enhancement as seen by the Textbox B.

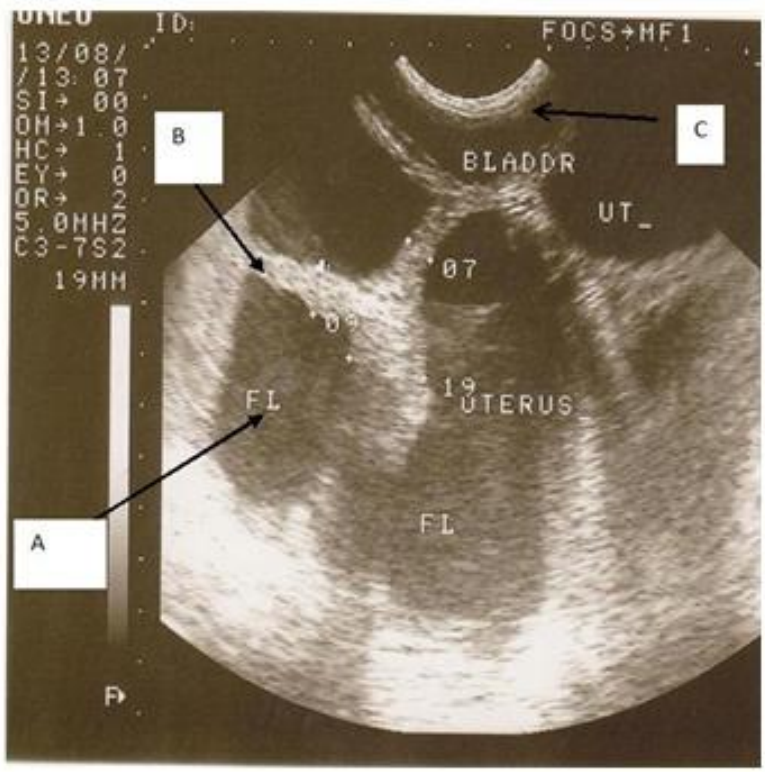

Figure 4. 16: Sonogram of the uterus of a dog diagnosed with pyometra A-uterine horn with pus. B-The hyperechoic margins are the uterine wall. C- The urinary bladder.

4.3.4 Uterine confirmatory tests

Diagnosis was determined by a combination of clinical signs and confirmatory tests. Presenting clinical signs reported were vomiting (1 case), a gradually enlarging abdomen (4 cases) and some purulent discharge from the vulva in four cases. Polyuria and polydipsia was also reported in one pyometra case.

A differential count of both cases revealed elevated neutrophil count (90%) and (88%) with a left shift noted on the haemogram. Other cell counts which included; Eosinophils, Basophils, Monocytes, and Lymphocytes, were within normal ranges. The case was confirmed on laparotomy with subsequent ovariohysterectomy the organ is seen in Figure 4.17 below.

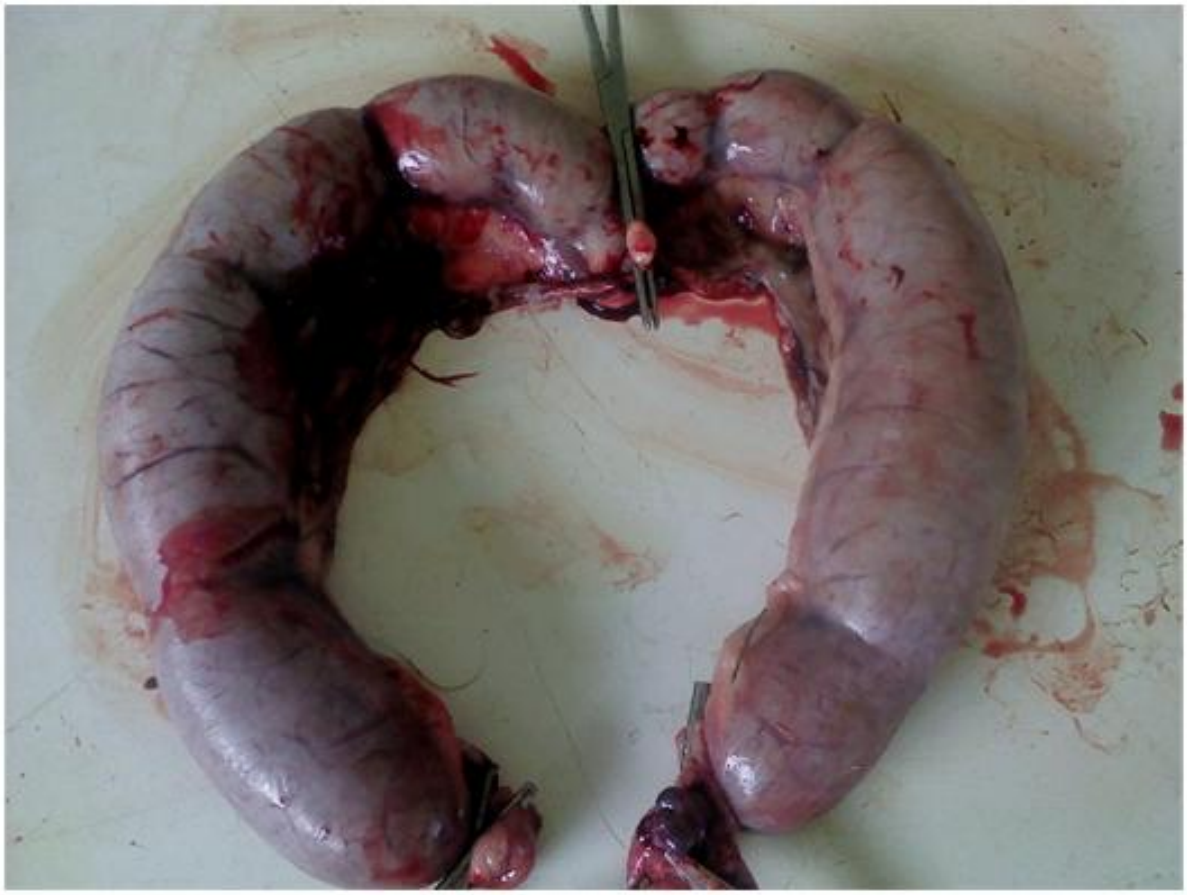

Figure 4. 17: Picture of the uterus with pyometra seen as distended uterine horns following ovariohysterectomy.

4.4 The urinary bladder

4.4.1 Normal anatomic location

The urinary bladder is located caudal to the umbilicus, from the midline to the inguinal region as seen in Figure 4.18. This is the scanning location for the bitch. In the male, due to the location of the *os penis,* the bladder is scanned lateral to the penile shaft.

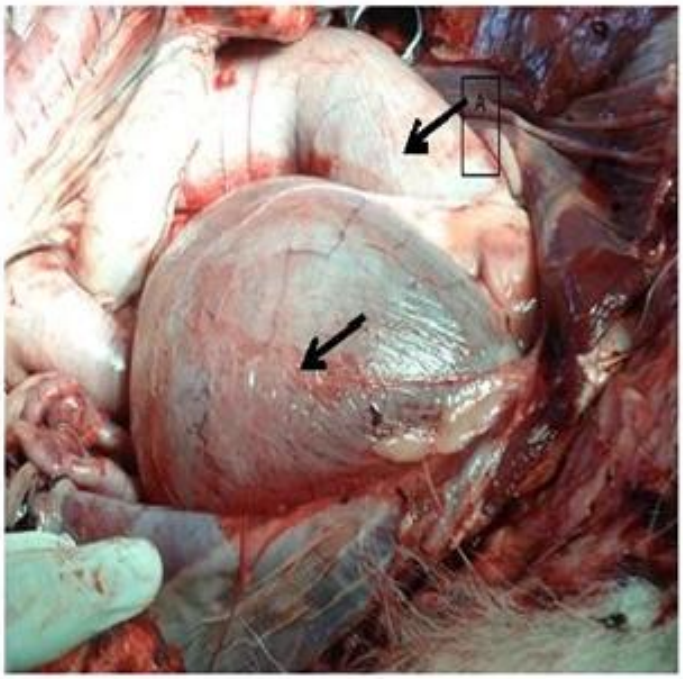

Figure 4. 18: Photograph of the urinary bladder position in dogs indicated by black arrow head A- colon.

4.4.2 Normal echotexture

The bladder contains urine which appears anechoic. Distal to this is a curvilinear area of echogenicity which is due to acoustic enhancement and caused by the fluid. Figure 4.12 shows the normal urinary bladder with a clearly demarcated floor on the right, and an ultrasound artifact formation known as pseudo-sludge making the bladder seem as if it has sediment.

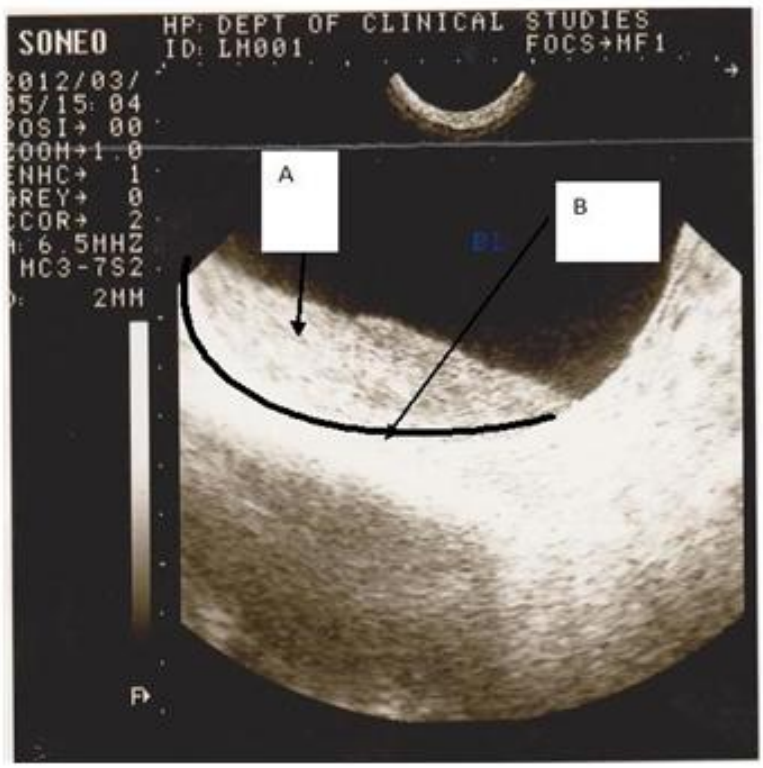

Figure 4. 19: Bladder sonogram A- pseudo-sludge artifact B- the true dorsal wall of the urinary bladder.

4.4.3 Sonographic findings of lesions of the urinary bladder

Figure 4.13 shows the sonogram of the urinary bladder with a white mass in the centre of the anechoic zone. The mass is a cystolith. The boundaries of the bladder are well delineated due to acoustic enhancement of urine. A clean acoustic shadow due to the cystolith depicted distally as a hypoechoic zone and which causes a gap in the region of acoustic enhancement.

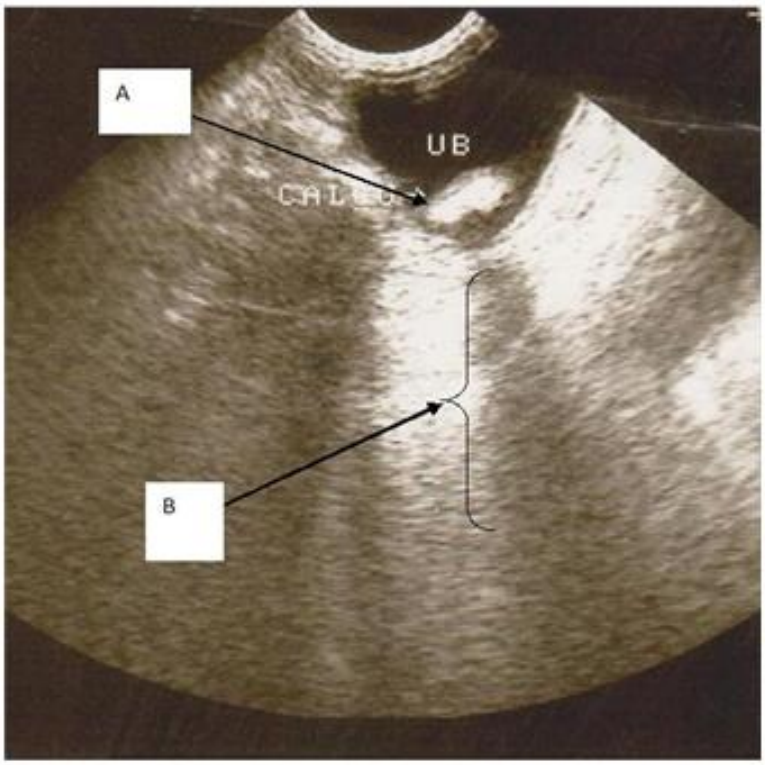

Figure 4. 20: Case 2 urinary bladder sonogram. A-bladder calculus, B-clear acoustic shadow.

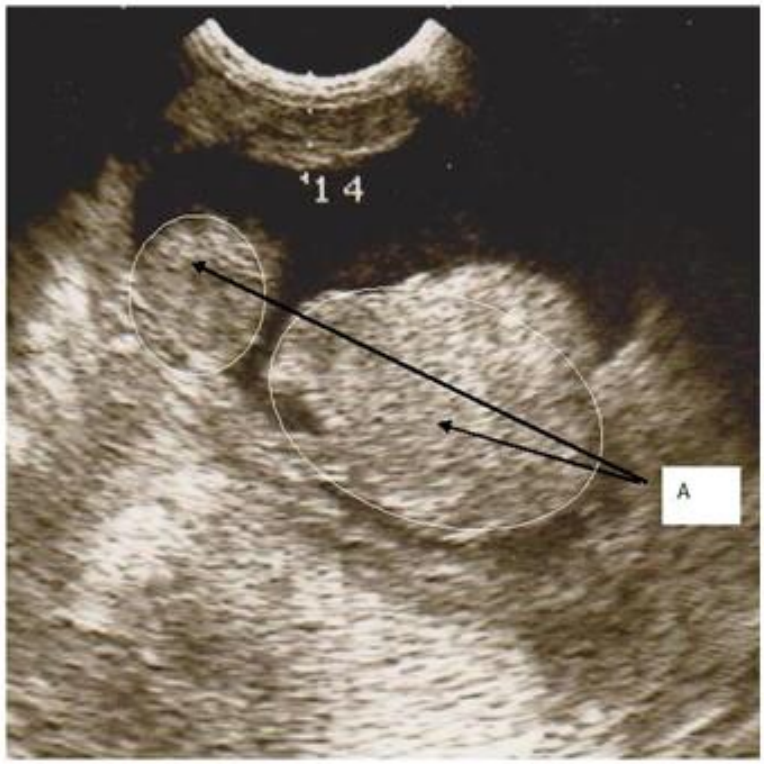

Figure 4. 21: a sonogram of a urinary bladder tumor (Case 15). A: tumor masses

Histopathological examination of the tumor mass found on post mortem in this case was determined to be a transitional cell carcinoma.

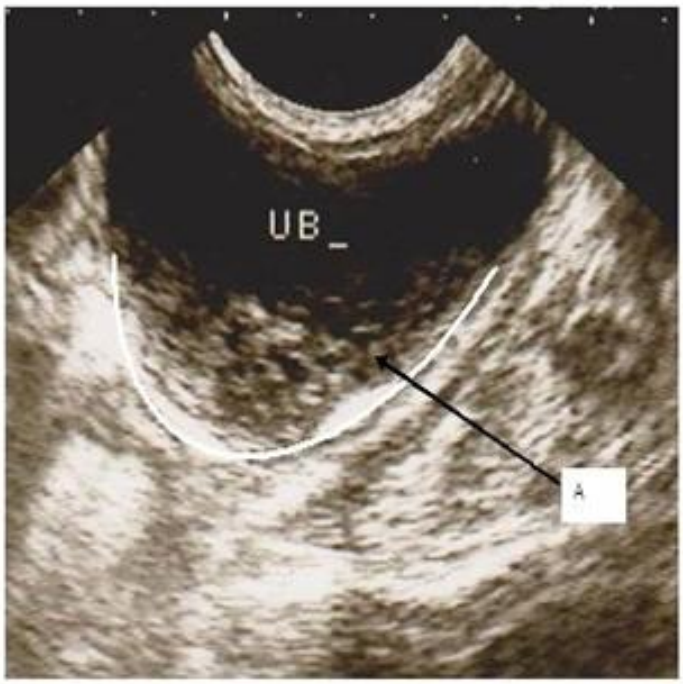

Figure 4. 22: A sonogram of urinary bladder (Case 13). UB- urinary bladder, A- the urinary bladder wall ventral border. The bladder has hyperechoic streaks due to urinary crystals (cystoliths).

4.4.4 Confirmatory tests of urinary bladder pathology

Diagnosis was determined by the use of clinical signs and other confirmatory tests. Clinical signs were reported in the following frequency for all four; urinary incontinence (two) and hematuria (three)

The additional confirmatory tests done included: urinalysis (two), radiography (three), exploratory laparotomy (two) and post-mortem with histopathology (one).

4.4.4.1 Dip stick urinalysis

The parameters analysed in dip stick urinalysis are as shown in Table 4.4.

Table 4. 4 Results of urinalysis from voluntarily voided urine obtained case 2.

Parameter	**Result**	**Normal**
Colour	Amber	Brown
Appearance	Turbid	Clear
Specific Gravity	1.025	1.016-1.060
pH	6	7.0-7.5
Protein	+	Nil
Glucose	Nil	Nil
Blood	++	Nil
Bilirubin	Nil	Nil
Urobilinogen	Nil	Nil

Key: + Low levels, ++ moderate levels, +++ high levels, Nil- negative results

The urine sample results revealed the following significant findings; presence of blood, protein, reduced pH, change of physical appearance and change in color. All these were indicative of disease.

Table 4. 5 : Results of microscopic examination of urine sample obtained from Case 2.

Parameter	**Result**	**Normal**
Sediment	Nil	nil
Epithelial Cells	++	Nil
Erythrocytes	+++	Nil
Leukocytes	+++	Nil
Casts	Nil	Nil
Granular	Nil	Nil
Bacteria	Nil	Nil
Crystals	Nil	Nil
Spermatozoa	Nil	Nil

Presence of epithelialelial cells, erythrocytes and leukocytes were indicative of disease in the sample.

4.4.4.2 Radiography

Radiography results of the dorsal ventral view of the abdomen revealed increased density of a rounded mass in the location of the urinary bladder as shown in Figure 4.16.

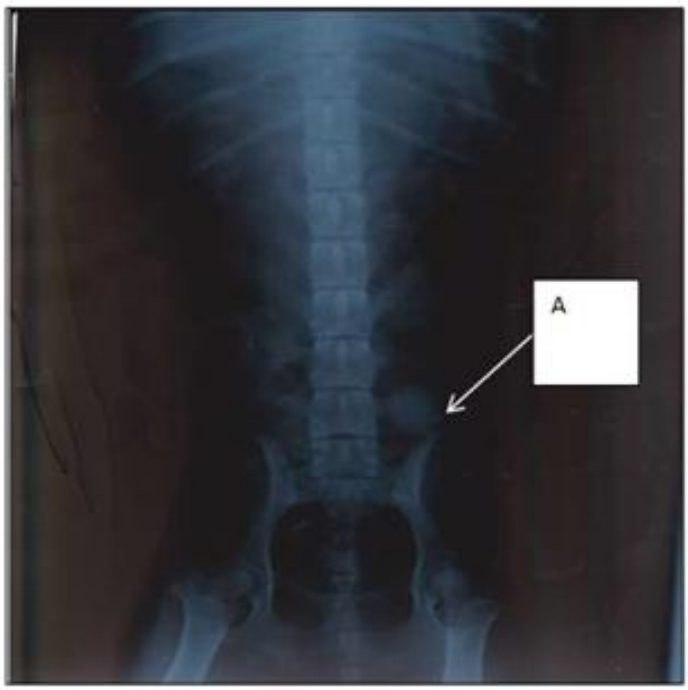

Figure 4. 23: Case 2 Radiographic dorso-ventral view of the pelvic abdomen showing a radiopaque mass in the bladder (A).

4.4.4.3 Exploratory laparotomy

Surgical exploration of Case 2 revealed the presence of a urolith in the urinary bladder, which was removed (Figure 4.24).

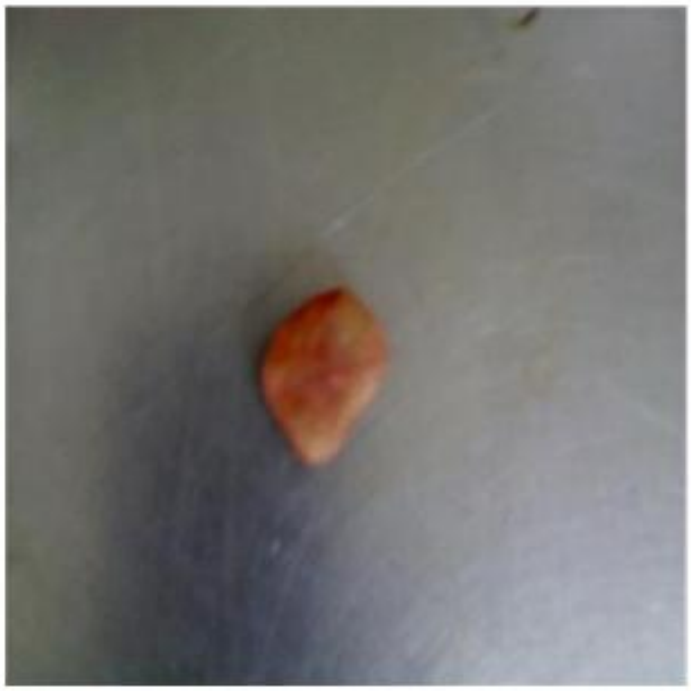

Figure 4. 24: The calculus recovered from the bladder which was determined to be Calcium phosphate.

The histopathology of the mass found on post-mortem on the urinary bladder revealed the mass to be a transitional cell carcinoma. Mitotic figures were seen in the sample with epithelialelial neoplastic cells also present. The photomicrograph of the same is seen in Figure 4.25 below.

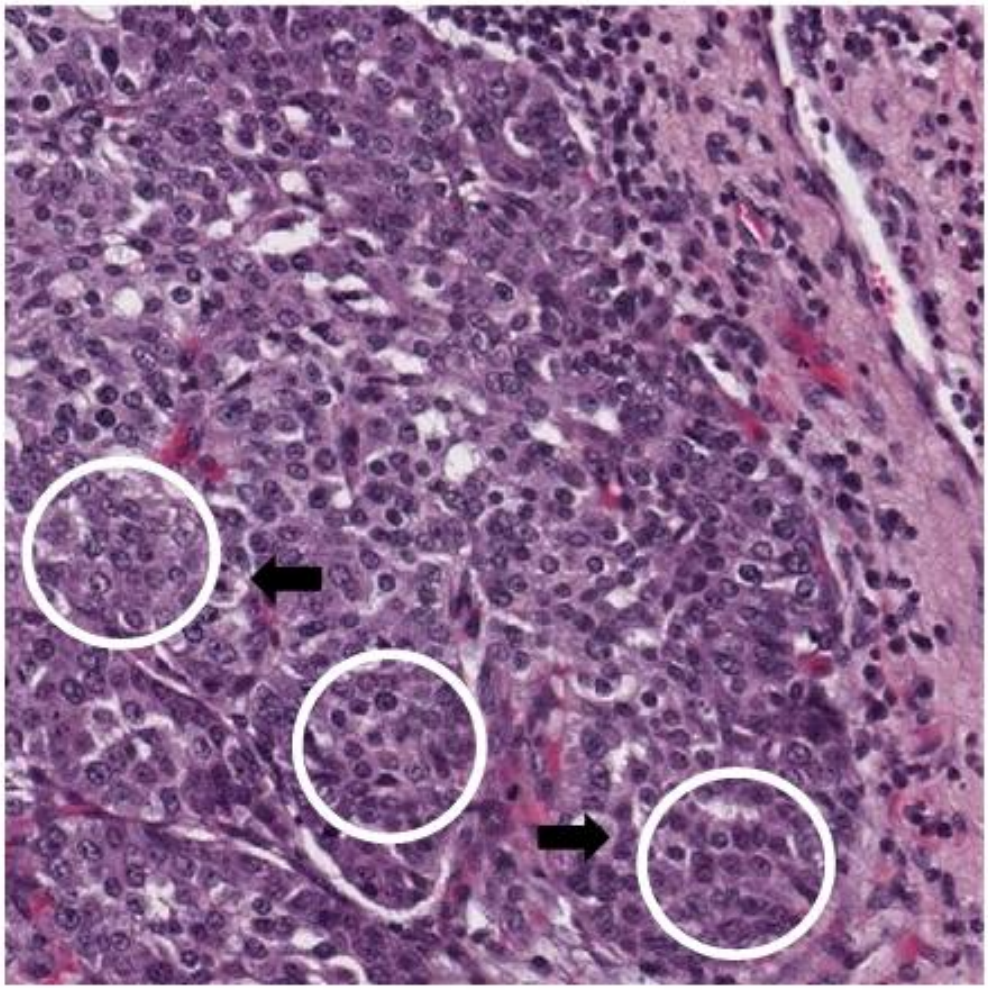

Figure 4. 25: Transitional cell carcinoma of urinary bladder mucosa: Islands of neoplastic epithelialelial cells (white circles) showing mitotic figures (black arrows) infiltrating the lamina propria.

4.5 Stomach

4.5.1 Anatomic location

The canine stomach is located on the left lateral aspect of the paralumbar fossa as seen in Figure 4.26. Its scanned position may expand due to its size as a result of its contents.

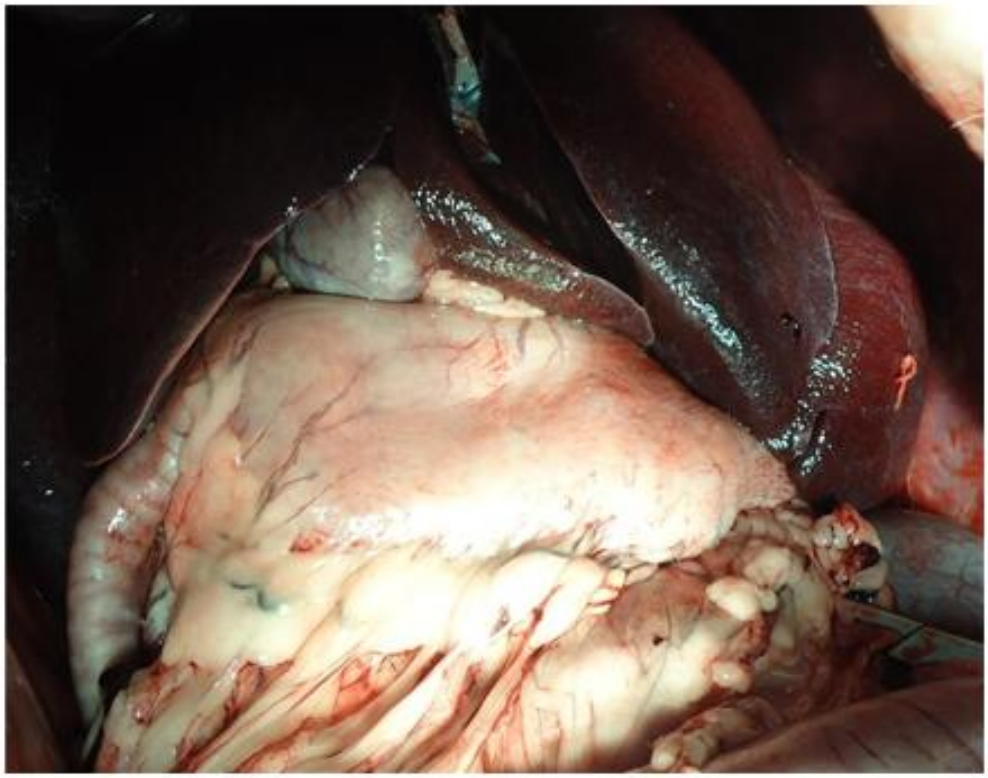

Figure 4. 26: Photograph of the approximate stomach position in a normal dogs following exploratory laparotomy.

4.5.2 Normal echotexture

The stomach may have contents such as fluid at the time of scanning which therefore gives the lumen an anechoic appearance (Figure 4.27). The stomach may also contain gas and this is seen as a dirty acoustic shadow distal to the mucosal gas interface which prevents visualization of distal parts of the stomach. It is recommended that dogs should be starved prior to scanning and water also given *ad libitum* to avoid this. Presence of ingesta will also lead to poor visualization due to the mixture of air, water and solid matter.

Figure 4.27 shows the stomach wall thickness measured using the internal callipers in the ultrasound machine. The stomach wall thickness is shown as 0.3cm. Note the acoustic enhancement distal to the stomach due to fluid accumulation in the stomach.

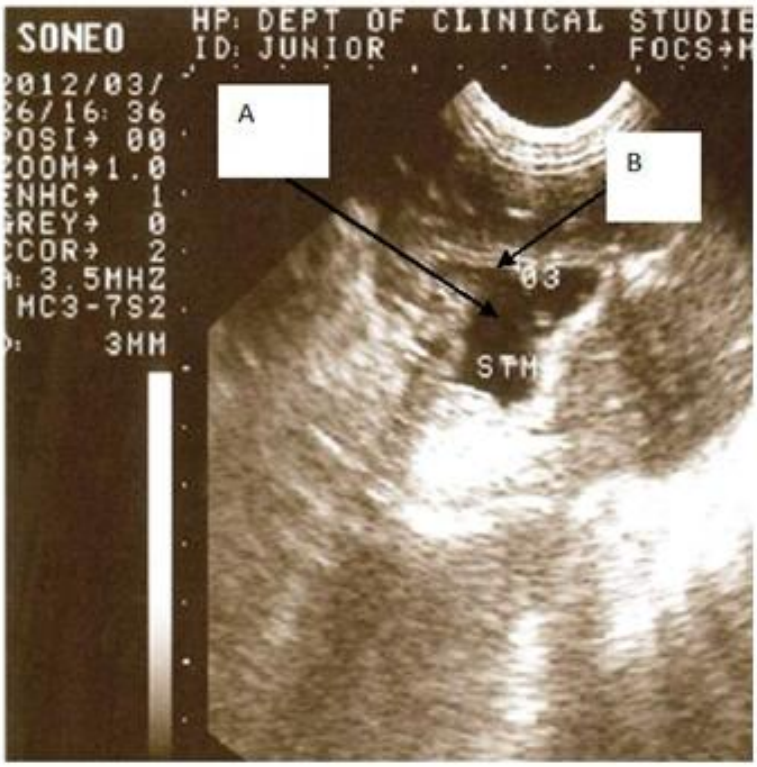

Figure 4. 27: Sonogram of the normal stomach of a dog. A-the stomach lumen with fluid. B-the stomach wall, note the two parallel lines denoting the thickness of the wall.

4.6 The intestine

4.6.1 Anatomic location

The intestines are demarcated as the duodenum, ileum and colon whose location is shown in Figure 4.28. The variation with regard to wall thickness of the various segments and location of these is reported by Agthe, (2009). However, it was not possible to replicate this during the study.

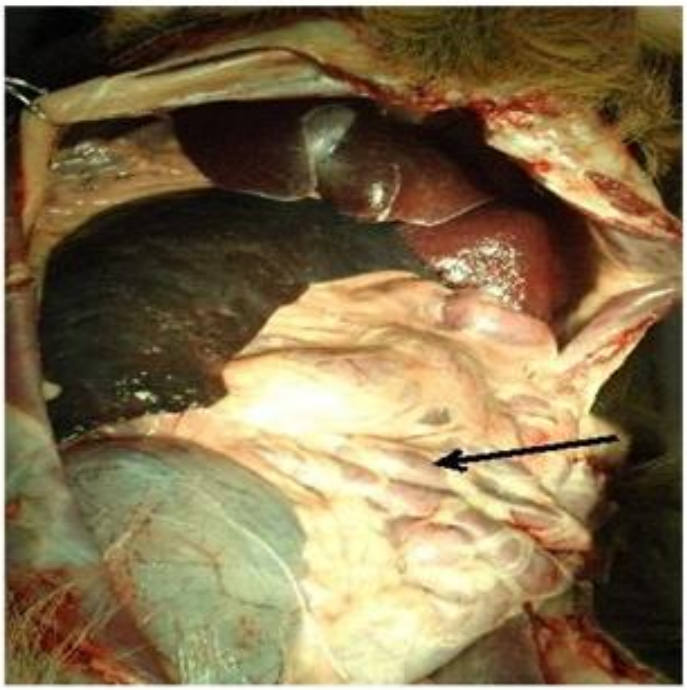

Figure 4. 28: Photograph of the normal intestinal tract in a normal dog location indicated by arrows. This was obtained from exploratory laparotomy.

4.6.2 Normal Echotexture

The intestinal architecture is noted as five clearly demarcated regions due to the structural composition of the wall. These are as follows: serosa, muscularis, submucosa, mucosa and mucosal-gas interface.

Figure 4.29 shows a longitudinal intestinal segment loop. Note the _blind end‘ as shown by the arrow end A. The dark curvilinear (anechoic) area is fluid within the intestinal segment.

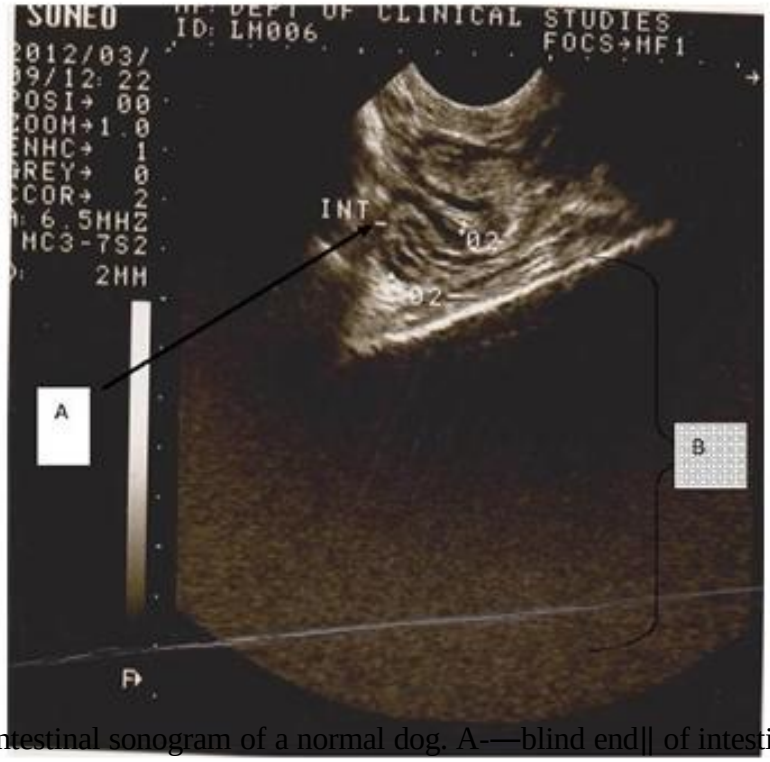

Figure 4. 29: Intestinal sonogram of a normal dog. A-—blind end|| of intestinal segment. The wall thickness is indicated as 0.2cm.

4.7 The spleen

4.7.1 The Normal location

Figure 4.30 illustrates the topographic location of the normal spleen, on the left paralumbar fossa, posterior to the costal arch. When small but of normal size, it may lie beneath the 12^{th} and13^{th} rib.

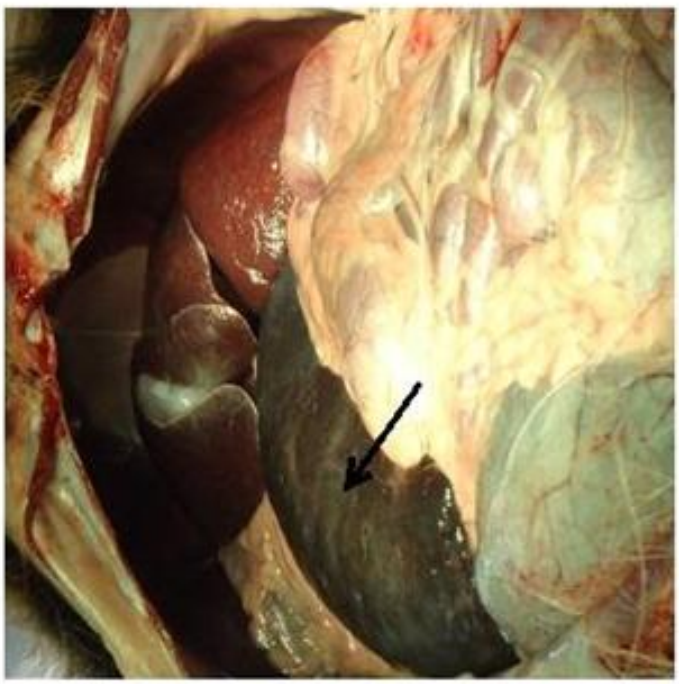

Figure 4. 30: Photograph of the position of the normal spleen in dogs obtained following exploratory laparotomy.

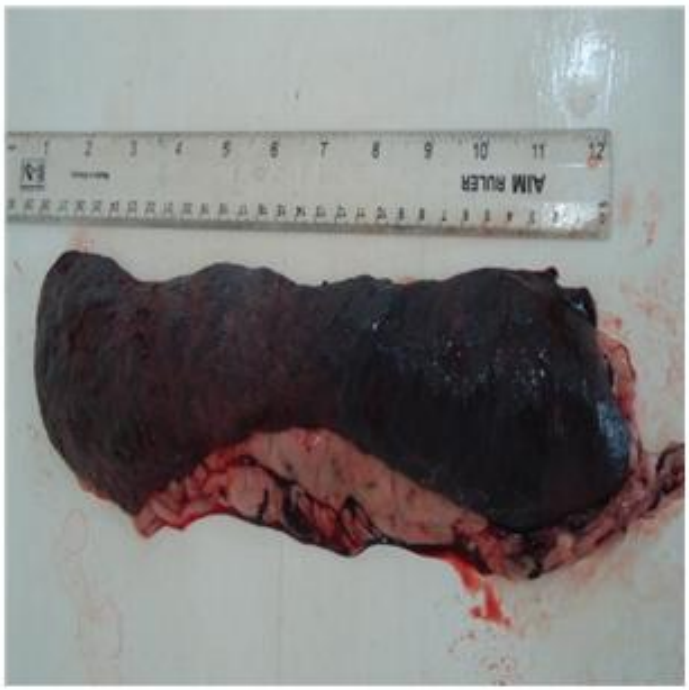

Figure 4. 31: Photograph of the normal spleen in a dog obtained following a post mortem.

4.7.2 Normal echotexture

The spleen appears as a fine grain texture which is homogenous throughout. The capsule of the spleen appears as a linear white line encompassing the organ. Figure 4.32 shows the spleen as a homogenous curvilinear mass on top of the image. A dark area is seen demarcating the splenic artery, which is a normal ultrasonographic finding in dogs.

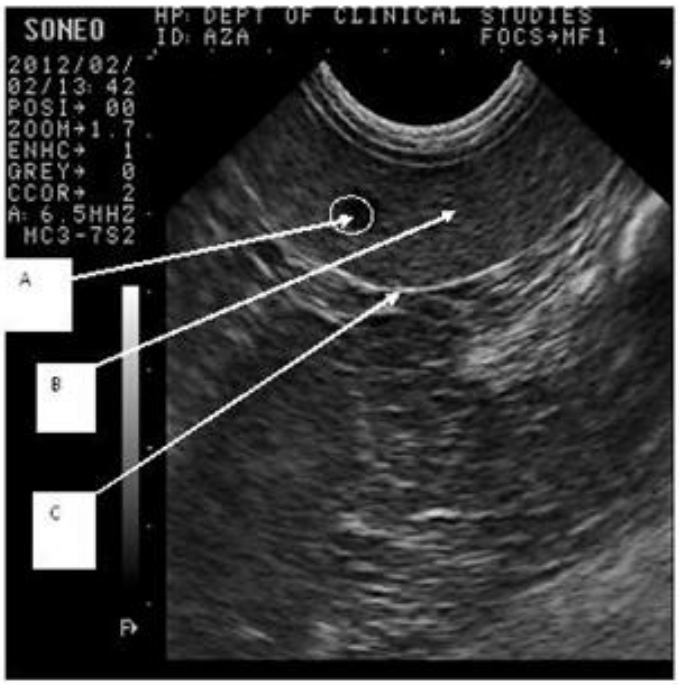

Figure 4. 32: Sonogram of a normal spleen in a dog A-Splenic artery, B-Splenic parenchyma, C-Hyperechoic wall of the spleen.

4.7.3 Results of pathologic splenic conditions

Two out of the twenty five cases 8% of the cases in the study group were splenic conditions. Both conditions were confirmed using histopathology as splenic hemangiosarcoma.

The ultrasonographic features of splenic hemagiosarcoma are presented in Figure 4.33. This was confirmed following post mortem and histopathological examination. The splenic mass was superimposed on the liver due to the proximity of the two organs which affected image interpretation. It was initially assumed that the mass was in the liver parenchyma. Figure 4.33 shows the mass as viewed on post mortem.

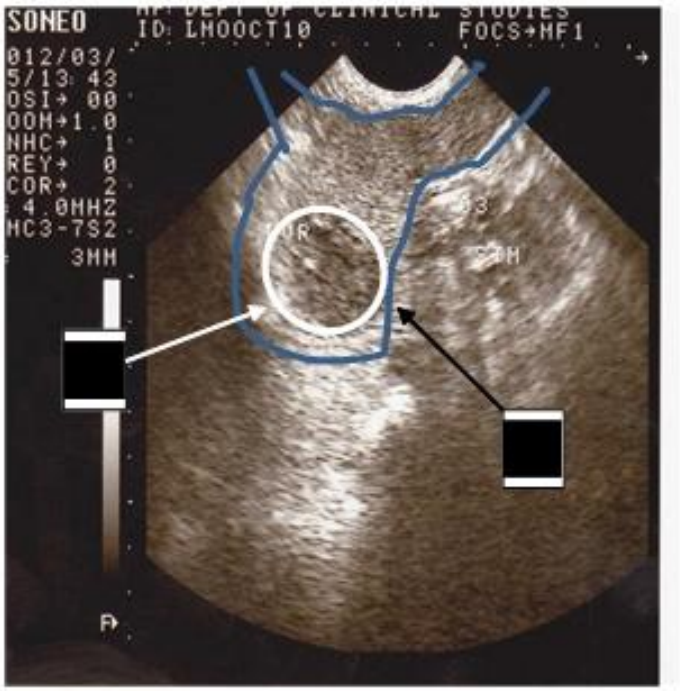

Figure 4. 33: Sonogram of the spleen in a dog diagnosed with hemangiosarcoma. Rounded mass superimposed on the liver structure A- the entire demarcation of the spleen, B- rounded splenic mass, STM-stomach wall.

4.7.4 Confirmatory tests of splenic pathology

The confirmatory tests for evaluation of splenic pathology were post mortem and histopathological examination. Figure 4.34 shows hemangiosarcoma which was confirmed by histopathology.

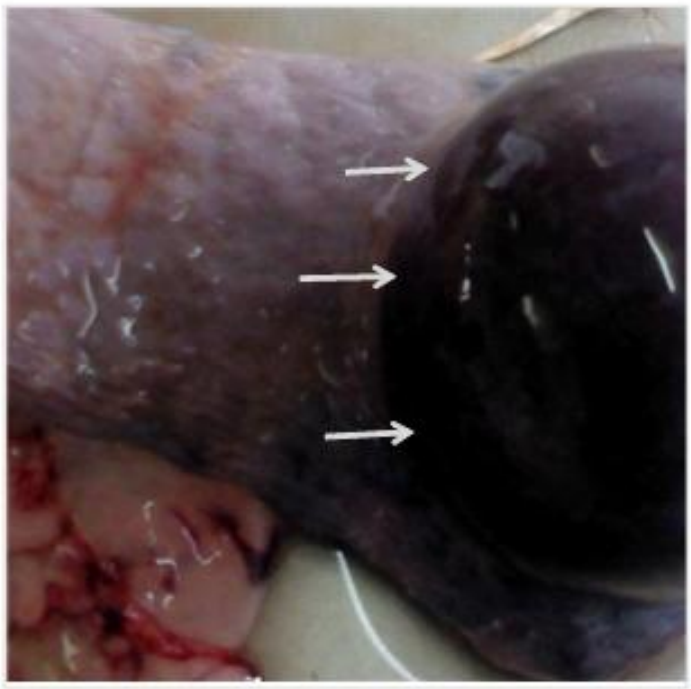

Figure 4. 34: Photograph of gross pathology of a spleen of a dog diagnosed with Splenic mass (Hemangiosarcoma). Gray arrows show the mass. The sample was obtained from post mortem.

The histopathology of the mass obtained from the post mortem was classified as a hemangiosarcoma. The findings of the photomicrograph are seen in Figure 4.35 demonstrating disruption in the histology of the spleen.

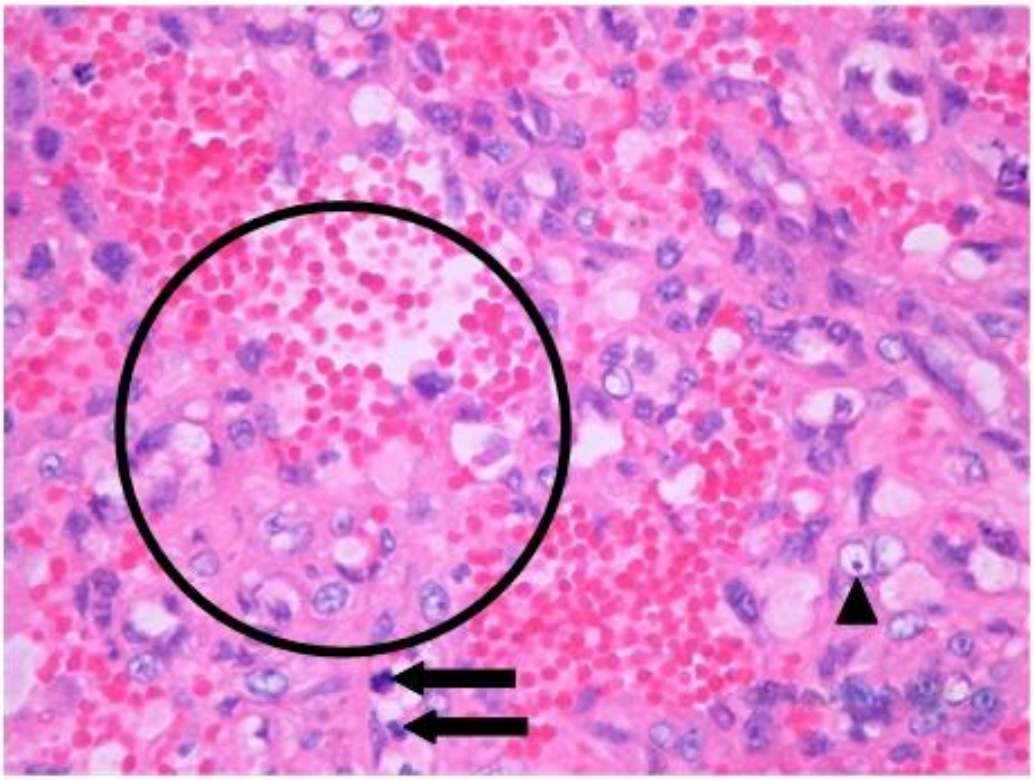

Figure 4. 35: Photomicrograph of splenic hemangiosarcoma; numerous round to polygonal cells with abundant eosinophilic cytoplasm arranged in sheets, some of which form blood-filled channels (black circle). The nuclei of some of these cells have dispersed chromatin and a prominent nucleolus (black arrow head). Mitotic figures were occasional (black arrows).

4.8 Quantitative analysis

Quantitative data on ultrasound measurements of the various organ dimensions was analysed and compared based on different breed types and age groups.

First, the animals were categorised into large and small breeds. It was observed that the average horizontal dimensions of the left kidney were larger than the corresponding dimensions of the right kidney when compared between all dog breeds. The left kidney horizontal average measurements of the small breeds were observed to be **5.07 (2.8-6.4)** cm, while that of the large breeds was observed to be **5.86 (4.7 -8.5)** cm as seen in Table 4.6.

It was also observed that the average horizontal dimensions of the left kidney were larger than the corresponding dimensions of the right kidney, when compared between all age groups. The left kidney measurements of dogs aged more than 1 year but less than 5 years had an average measurement of **4.82 (2.8- 6.10)** cm, dogs aged more than 5years but less than 10 years had an average measurement of **5.7 (3.7-8.5)** cm and dogs aged more than 10 years had an average measurement of **6.04 (5.3-6.9)** cm as seen in Table 4.7.

However, incomplete visualization of the right kidney attributed to its anatomical location contributed to reduced accuracy in the right kidney dimensions.

Table 4. 6 : Averages of organs based on dog breed taken from sonogram measurements.

Breed	Lk (h)	Lk (v)	Rk (h)	Rk (v)	Swt	Sit
1	5.07	2.99	4.89	2.86	0.3	0.3
2	5.86	3.42	5.03	3.17	0.34	0.34

Key: 1: Small breed dogs, **2**: Large breed dogs ; **Lk(h)-** left kidney horizontal diameter, **Lk(v)**- left kidney vertical diameter, **Rk(h)**- right kidney horizontal diameter, **Rk(v)**- right kidney vertical diameter, **Swt**- stomach wall thickness, **Sit**- intestinal wall thickness.

Table 4. 7: Averages of organs based on age taken from sonogram measurements.

Age	Lk (h)	Lk (v)	Rk (h)	Rk (v)	Swt	Sit
B	4.82	2.94	4.31	2.91	0.32	0.29
C	5.7	3.22	5.28	2.95	0.32	0.32
D	6.04	3.5	5.23	3.15	0.3	0.32

Key: B: >1year to < 5 years, **C** :> 5years to <10 years **D**: >10 years; **Lk(h)-** left kidney horizontal diameter, **Lk(v)**- left kidney vertical diameter, **Rk(h)**- right kidney horizontal diameter, **Rk(v)**- right kidney vertical diameter, **Swt**- stomach wall thickness, **Sit**- intestinal wall thickness.

The vertical dimensions of the left kidney were also assumed to be larger than the corresponding dimensions of the right kidney as seen in Table 4.7. Upon t-test analysis, it was found that a P value of 0.02 was obtained for large dogs for the left and right

kidney horizontal measurements. This confirmed a statistically significant difference between the horizontal measurements of the left and right kidney for large dog breeds. P values for the different organ parameters were found to have no significant difference between breeds and age groups as shown in Tables 4.8 and table 4.9 respectively. This was best visualized in Figures 4.27 and 4.28. The thickness of the stomach wall and intestinal wall were observed to remain relatively constant in the different breeds and age groups as shown in Tables 4.7 and 4.8.

Table 4. 8: P values of sonogram measurements based on dog breed.

Parameter	**P-value**
Lkh1 vs Rkh1	0.30
Lkh2 vs Rkh2	**0.02**
Lkv1 vs Rkv1	0.21
Lkv2 vs Rkv2	0.21
Sw1 vs Sit1	0.79
Sw2 vs Sit2	0.60

Note: P-values not highlighted were not significant as they were greater than 0.05.

Key: 1: Small breed dogs, **2**: Large breed dogs **Lkh**- left kidney horizontal diameter, **Lkv**- left kidney vertical diameter, **Rkh**- right kidney horizontal diameter, **Rkv**- right kidney vertical diameter, **Sw**- stomach wall thickness, **Sit**- intestinal wall thickness.

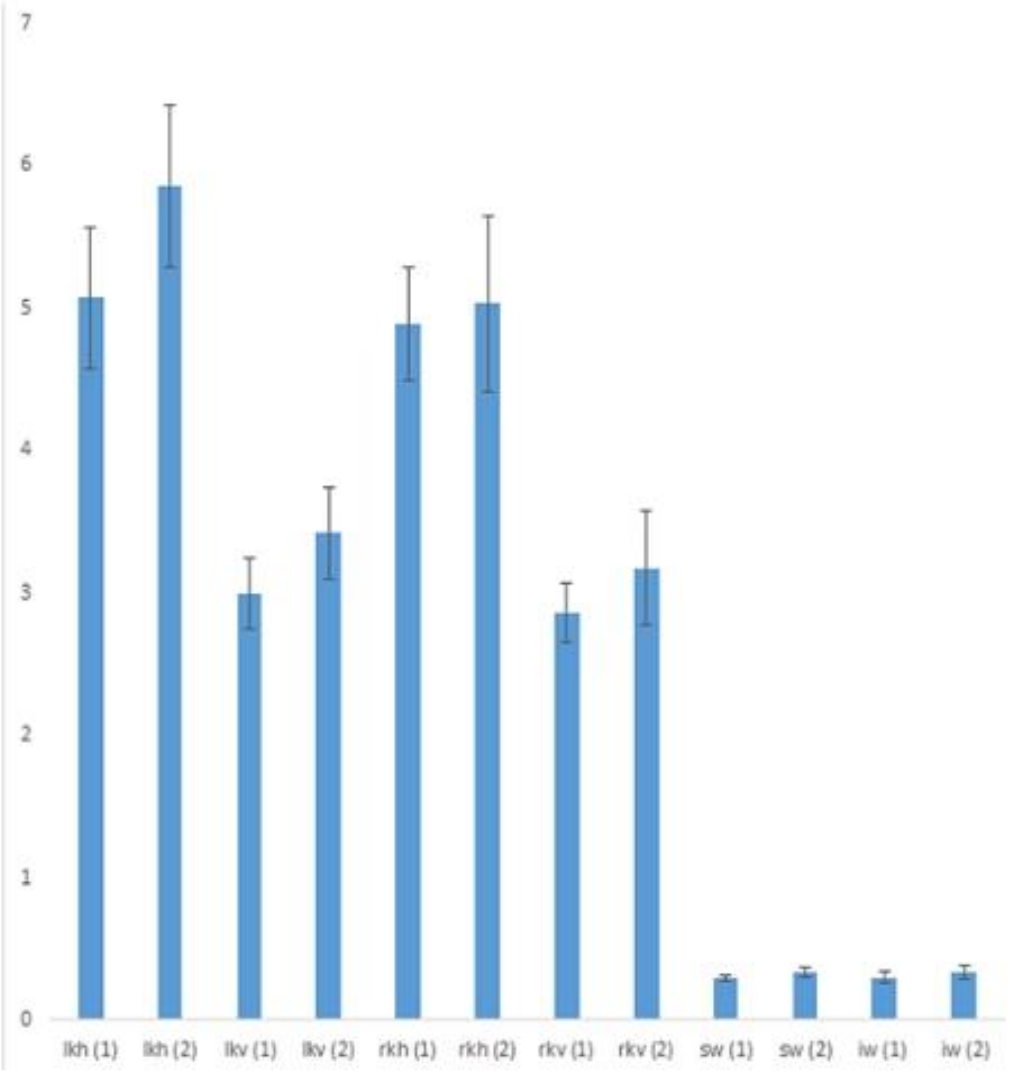

Figure 4. 36: 95 % confidence level of sonogram measurements based on dog breed.

Table 4. 9: P values of sonogram measurements based on dog age.

Parameter	P-Value
Lkh(b) vs Rkh(b)	0.11
Lkh (c)vs Rkh (c)	0.36
Lkh(d) vs Rkh(d)	0.21
Lkv (b) vs Rkv (b)	0.32
Lkv (c) vs Rkv (c)	0.40
Lkv (d) vs Rkv(d)	0.11
Sw (b) vs Sit (b)	0.53
Sw (c) vs Sit (c)	0.79
Sw (d) vs Sit (d)	0.39

Note: All P-values were not significant as they were greater than 0.05

Key: b: >1year to < 5 years, **c** :> 5years to <10 years **d**: >10 years; **Lkh**- left kidney horizontal diameter, **Lkv**- left kidney vertical diameter, **Rkh**- right kidney horizontal diameter, **Rkv**- right kidney vertical diameter, **Sw**- stomach wall thickness, **Sit**intestinal wall thickness.

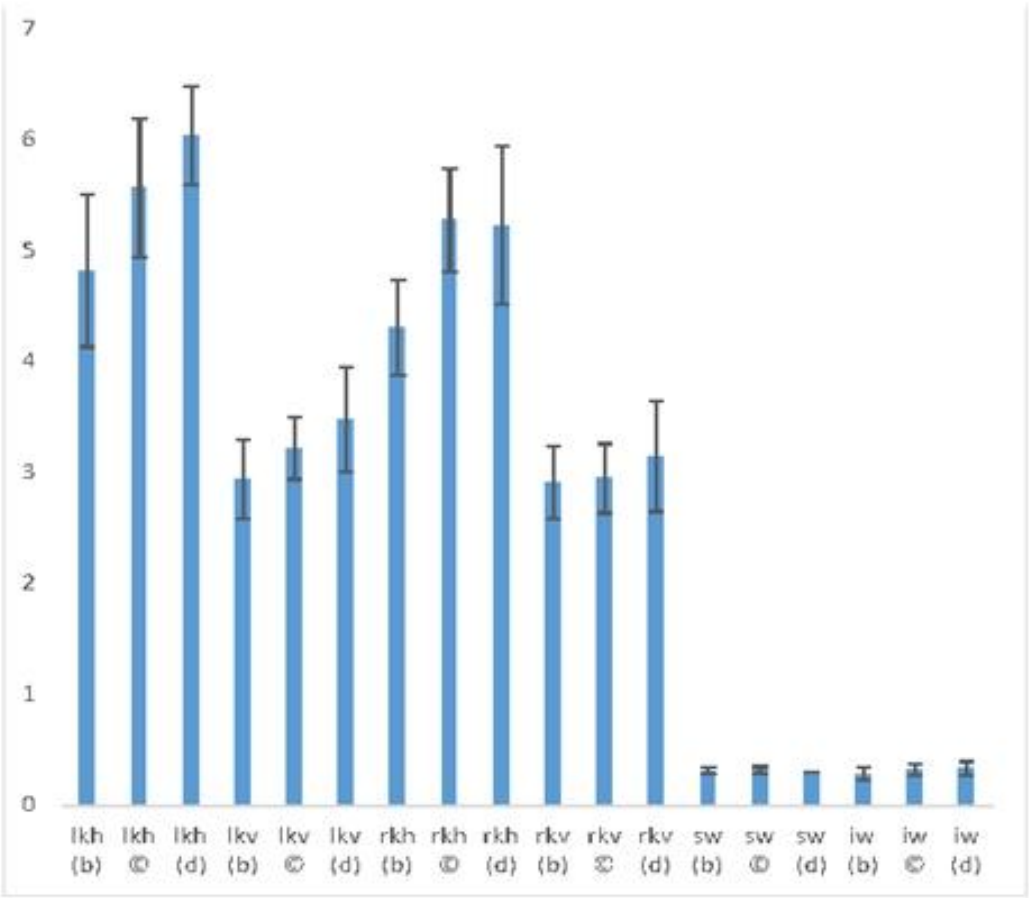

Figure 4. 37: 95 % confidence level of sonogram measurements based on dog age

Following the ultrasound examination and ancillary tests, the medical and surgical management was done on a case by case basis. Humane euthanasia following owners consent was done for patients with poor prognosis.

CHAPTER FIVE: DISCUSSION, CONCLUSIONS AND RECOMMENDATIONS

5.1 DISCUSSION

The study aimed at highlighting how ultrasound can be used to diagnose abdominal disease conditions in dogs. It represents the first original work describing clinical and ultrasonographic features of some abdominal disease conditions in dogs in Nairobi area, Kenya. The study findings helped provide an overview of some of the abdominal disease conditions encountered by clinicians and described how ultrasound could be used as a confirmatory test in the diagnosis of the same.

Previously, abdominal disease conditions were only subjected to one diagnostic imaging technique for confirmation, mainly radiography. This did not provide much information especially where soft tissue pathologies were involved. The limited use of ultrasound as an imaging technique in Kenya has been hindered largely due to lack of expertise in the technique among veterinary surgeons and the high cost of the ultrasound machines. This has recently changed with the advent of portable and affordable ultrasound machines. However, the uptake of the technique by veterinary surgeons is still low due to the lack of technical expertise in the use of the machine and image interpretation. The study aimed at enhancing the use of ultrasonography in the diagnosis of abdominal disease conditions through image presentation of some abdominal conditions as well as image interpretation.

It was noted that most of the cases presented were referrals from other clinics with poor prognosis. This was majorly attributed to the unavailability of an array of confirmatory tests, which could be carried out. The most frequent clinical signs presented included anorexia, with loss of condition which was reported in all twenty five cases (100%) of the cases reported. However, it was also noted that some signs involved several organ systems. In such cases, a minimum data base of the most significant findings was used

to come up with a tentative diagnosis of the organ system most likely to be involved and to identify the condition.

It was observed that there was a high population of male animals compared to female animals presented with abdominal disease conditions. In addition, all twenty five (100%) of the animals sampled were above the age of 1 year with 30% in the between 2-5 years of age.

Liver disease was the most common pathological condition identified in this study (20%). It presented with a history and clinical signs of progressive abdominal enlargement. The abdomen was reported as being pendulous and on palpation revealed presence of fluid. The echotexture of the normal liver parenchyma was reported to have heterogenous echogenicity with hyperechoic portal vein walls and anechoic gall bladder lumen. Liver disease most commonly reported was cirrhosis which was observed as hyperechoic parenchyma with small areas of hypoechoic regions. These changes were seen to vary depending on the severity of the disease. This is similar to what was reported by other authors Barr (1988); Besso *et al (*2000); Cruz-Arambulo (2003) and Lamb (1995). It was thought that the relation to the high liver pathology incidence was attributed to the high incidences of aflatoxicosis as most of the commercial feeds in Kenya are processed using maize.

The horizontal kidney dimensions revealed a significant difference between the right and left kidneys with the left being larger. Similar findings were also reported by Eshar *et al.* (2013) and Lamb (1995). Other findings on kidney dimensions were seen by Barella *et al.* (2012) who correlated the kidney dimensions to the lumbar vertebral length of L5 and L6 and found no difference in the kidney dimensions. In addition, the echotexture of the hydronephronic kidney observed in the study group and seen as dilated renal pelvis filled with anechoic fluid was similar to that reported by Lamb

(1988). The exact kidney measurements have not been established but ranges of these measurements are given by Lamb (1995) and Barella *et al.* (2012).

Splenic conditions reported in the study group were two, both of which were classified histologically as splenic hemangiosarcoma. The lesions were observed as increased echogenicity of the lesion area with a distorted parenchyma echotexture. The two conditions presented with varied severity and the histopathology. However it was important to note that the presence of neoplastic changes were evident. The description of the ultrasonographic features of the diseased splenic conditions was similar to those reported by (Lamb 1988). The histopathology of the lesions confirmed splenic hemangiosarcoma.

The uterus was examined in all female animals presented for both the study and the control group. Two conditions were reported in the study group; these were pregnancy and pyometra. For this study, pregnancy was reported as a finding to report the normal ultrasonographic features of pregnancy. Pregnancy was described as visualization of gestational sacs with anechoic fluid and hyperechoic foetal skeleton surrounded by hypoechoic soft tissue of foetal parts. This is similar to findings reported by Lamb (1988) and Lamb (1995). The non-gravid uterus in the female control animals could not be visualised as is similarly reported by Lamb (1988) and Lamb (1995).

Intestinal and stomach wall thickness recorded throughout the control group showed no significant difference in the dimensions when compared between breed and age groups. Bradley (2005) and Lamb (1995) found similar ranges in the dimensions of the gastrointestinal tract. The ultrasonographic appearance of the intestinal tract wall was observed as a hyperechoic serosa, a hypoechoic muscularis, a hyperechoic sub-mucosa, a hypoechoic mucosa and hyperechoic mucosa-lumen interface. This gave the wall a double lined appearance. This echotexture was also reported by Agthe (2009) and Lamb

2007). Gas interference was observed to affect clarity of the images and hindered the accurate measurement of some intestinal segments; this was also reported by Barr (2007); Lawson and Biller (2009).

The study showed that ultrasound was reliable as a confirmatory diagnostic test in cases where the gross changes could be determined. It was also used in combination with other tests to determine changes in physiological function. It was also possible to evaluate organs in different stages of gross damage all with varying functional damage.

The study was able to identify the various confirmatory tests available to practitioners in the diagnosis of abdominal disease and the limitations of each based on availability and costs. The use of ultrasound as an added confirmatory test to this range of available confirmatory tests would widen the scope of diagnosis. It was noted that in some cases, the confirmatory tests selected such as exploratory laparotomy, required patient stabilization prior to surgery which increased the duration of recovery.

Though ultrasound descriptions were similar to other author‘s findings Lamb ($1990_{1)}$ and Lamb (1995), the ancillary tests carried out varied on a case by case basis. The images seen on the scanner screen will vary between operators. However, the most important aspect of sonography is knowledge of the normal echotexture of an organ in order to know when there is presence of abnormalities. In some organs such as the liver, urinary bladder and kidney, clinical signs are seen usually after extensive damage to the entire organ. Ultrasound is able to detect minute changes in the echotexture and aid in diagnosis.

5.2 CONCLUSIONS AND RECOMMENDATIONS

5.2.1 CONCLUSIONS

The study came up with the following conclusions:

1. The clinical signs exhibited were able to be related to the ultrasonographic findings in all the cases presented with abdominal disease.
2. The diseased and normal organs showed clear variations in their echotexture with changes seen varying from mild to severe.
3. Diagnoses reached using the ultrasound findings of the study group were corroborated by the ancillary tests carried out for each case in the study group.
4. Organ measurements remained relatively similar between varied ages and breed types. However variations were noted between the horizontal diameters of the left kidney when compared to the corresponding measurement of the right kidney. The left kidney was found to be longer.

Therefore, the use of ultrasound at the University of Nairobi, Small Animal Clinic for the diagnosis of abdominal disease has aided in the understanding of abdominal disease conditions. In addition, it is safe, quick and easy to use and has improved the patients' wellbeing through prompt diagnosis which in turn leads to better patient management.

5.2.2 RECOMMENDATIONS

1. Further training in ultrasonography through Continuous Professional Development (CPD) programs will empower veterinarians with knowledge and increase their exposure to ultrasound in the diagnosis of abdominal disease. This will translate to added diagnostic imaging options available for the management of their cases.
2. It is recommended that ultrasound should be used in the confirmatory diagnosis of abdominal disease conditions in dogs.
3. Further research should be done on how the measurements of organs could be used for diagnosis of abdominal disease conditions.

CHAPTER SIX: REFERENCES AND APPENDICES

6.1 REFERENCES

Agthe P., (2009): Ultrasonography of the gastrointestinal tract and associated organs in dogs and cats. In Practice **31:** 182-188.

Barella. G., Lodi M., Sabbadin L. A. and **Faverzani S., (2012)**: A new method for ultrasonographic measurement of kidney size in healthy dogs. Journal of Ultrasound **15:** 186-191.

Barr F.,(1988): Diagnostic ultrasound in small animals. In Practice **10:** 17-25.

Barr F.,(2007): Getting the best reults from ultrasonography. In Practice **29:** 520-525. **Besso J. G., Wrigley R. H., Gliatto J. M.** and **Webster C. R. L., (2000):** Ultrasonographic appearance and clinical findings in 14 dogs with gallbladder mucocele. Veterinary Radiology and Ultrasound **41:** 261-271.

Boswood A. and **Lamb C., (2005)**: Doppler ultrasound examination in dogs and cats: 3. Assessment of cardiac disease. In Practice **27:** 286-292.

Bradley K. (2005): Practical contrast radiography 2. Gastrointestinal studies. In Practice **27:** 412-417.

Burk R. and **Feeny D.,(2003):** Small animal radiology and ultrasonography : A diagnostic atlas and text, (3rd Ed) Saunders. St. louis. missouri. USA pg 249-466.

Cartee R.E., (1995): Practical Veterinary Ultrasound. Williams & Wilkins Media, Pennsylvania, USA

Choi J., Kim, H. and **Yoon J., (2011**): Ultrasonographic adrenal gland measurements in clinically normal small breed dogs and comparison with pituitary-dependent hyperadrenocorticism. Journal Veterinary Medicine Science **73:** 985-9.

Cruz-arámbulo R. and **Wrigley R., (2003):** Ultrasonography of the acute abdomen. Clinical Techniques in Small Animal Practice **18:** 20-31.

Dyce K. M., Sack W. O. and **Wensing C. J. G. (Eds) (1996):** The abdomen of the Carnivores In Textbook of Veterinary Anatomy. 2nd Ed . W.B Saunders Co. Philadephia USA.

Eshar D., Briscoe J. A. and **Mai W., (2013):** Radiographic kidney measurements in North American pet ferrets (Mustela furo). Journal of Small Animal Practice 54: 15-9.

Freeman S., (2002): Ultrasonography of the equine abdomen: techniques and normal findings. In Practice, **24:** 204-211.

Hanazono K., Fukumoto S., Endo Y., Ueno H., Kadosawa T. and **Uchide T. (2013):** Ultrasonographic findings related to prognosis in canine Transitional Cell Carcinoma. Veterinary Radiology and Ultrasound. **55**(1): 79-84.

Hayward N., (2006): Practical guide to imaging abdominal masses. In Practice, **28:**84-93.

Lamb C. R., (1990_1): Abdominal ultrasound in Small Animals: Examination of the liver, spleen and pancreas. Journal of Small Animal Practice **31:** 6-15.

Lamb C. R., (1990_2): Abdominal ultrasound in Small Animals: Intestinal tract and Mesentery, kidneys, adrenal glands, uterus and prostate. Journal of Small Animal Practice **31:** 295-304.

Lamb C.R., (1995): Abdominal Ultrasound in Small animals In "Veterinary Ultrasonography" Goddard, P. J., (Ed) CAB International. Wallington UK pg 21-54.

Lamb C. R., (2005): Doppler ultrasound examination in dogs and cats: 2. Abdominal applications. In Practice **27:** 238-247.

Lattimer J., (2000): The expanding role of ultrasonography in everyday practice. Veterinary. USA.

Lattimer S. K., Mahaffey A. E. and **Prasse W. K. (2003):** Duncan and Prasse's Veterinary Laboratory Medicine:Clinical Pathology 4th ed. Willey 2003. Missouri USA.

Larson M. M. and Biller D. S., (2009): ultrasound of the gastrointestinal tract. Veterinary Clinics of North America Small Animal practice **39**: 747-759.

Lisciandro G.R., (2011). Abdominal and thoracic focussed assessment with sonography for trauma, triage and monitoring in small animals. Journal of Veterinary Emergency and Critical care **21**: 104-122.

Kirberger R. M., (1995): Imaging Artefacts in Diagnostic Ultrasound—A Review. Veterinary Radiology and Ultrasound **36:** 297-306.

Sharma A., Thompson M. S., Scrivani P. V., Dykes N. L., Yeager A. E., Freer S. R. and **Erb H. N., (2011)**: Comparison of radiography and ultrasonography for diagnosing small-intestinal mechanical obstruction in vomiting dogs. Veterinary Radiology and Ultrasound **52:** 248-55.

Tams, T.,(2003): Handbook of small animal gastroenterology, Saunders. St. Louis Missouri USA.

Watson P. J., Archer J., Roulois A. J., Scase T. J. and **Herrtage M. E., (2010):** Observational study of 14 cases of chronic pancreatitis in dogs. Veterinary Record **167:** 968-976.

World Health Oorganisation 1998: Training in diagnostic ultrasound: essentials, principles and standards. Report of a WHO Study Group. World Health Organ Tech Rep Ser, 875.

6.2 APPENDIX

Appendix A: control group summary

case no	Age	Weight in Kgs	Breed type	Sex	Left kidney dimensions		Right kidney dimensions		stomach wall thickness	intestine wall thickess
					horizontal diameter	vertical diameter	horizontal diameter	vertical diameter		
CT1	C	40	2	M	5.6	3.9				0.2
CT2	C	18.1	1	M	3.9	2.9			0.3	0.3
CT3	C	28.3	2	M	8.5	4.3	6	3	0.3	0.3
CT4	C	24.3	2	F	5.3	3.5			0.4	0.3
CT5	B	9.6	1	M	4.1	2			0.3	0.2
CT6	C	14.1	1	M	5.8	3.5	4.6	2.3	0.4	0.2
CT7	B	11.7	1	M	5.5	3.2	3.9	2.3		
CT8	B	15.7	1	F	5.7	3.1	5.2	3.3	0.3	0.3
CT9	C	28.8	2	M	6.3	3.6	5.8	3.3	0.4	0.4
CT10	C	23.8	2	M	4.7	3.1	4.9	3.9	0.3	0.4
CT11	C	14.5	1	M	5.8	2.5	4.6	3.3	0.3	0.3
CT12	C	12.8	1	M	5.5	3.2	3.9	2.3	0.3	0.2
CT13	D	17.8	1	M	5.7	2.6	5.6	2.6	0.3	0.4
CT14	C	10	1	M	6.1	3.2	6.1	2.8		0.4
CT15	D	39.7	2	M	6.9	4	3.9	2.9		0.2
CT16	D	17	1	M			4.4	2.8	0.3	0.2
CT17	B	25.6	2	M	3.6	2.5	3.2	2.2	0.3	0.4
CT18	B	20.9	2	F	5.8	3.4	4.1	3	0.4	0.2
CT19	C	19.5	1	M	3.7	2.9	5.8	3.1	0.2	0.3
CT20	C	21.36	2	M	6.1	2.9	6.2	3.2	0.3	0.5
CT21	D	30.45	2	M	5.6	3.3				0.4
CT22	D	27	2	M	6.8	4.6	6.3	4.5		0.3
CT23	B	23.63	2	M	6.1	3.5	5	3.4		0.3
CT24	B	16.36	1	F	4.9	3.7	4.3	3.5		0.3
CT25	B	10	1	F	4.9	2.8	4.8	3.1	0.3	0.2
CT26	D	20	1	M	5.3	3.8	5	3.1	0.3	0.4
CT27	D	9.09	1	M	6.4	3.2	6.2	3	0.3	0.4
CT28	B	7.8	1	M	2.8	2.3	4	2.5	0.3	0.4
CT29	D	23.63	2	M	5.6	2.9				0.4
CT30	C	27.27	2	M	5.1	2.4	4.9	2.3	0.3	0.4

Appendix B: 95 % confidence calculation for sonogram measurement comparisons at different dog ages

lkh(b)	lkhc	lkhd	lkvb	lkvc	lkvd	rkhb	rkhc	rkhd	rkvb	rkvc	rkvd	swb	swc	swd	iwb	iwc	iwd	
4.1	5.6	5.7	2	3.9	2.6		6	5.6			2.6	0.3		0.3	0.2	0.2	0.4	
5.5	3.9	6.9	3.2	2.9	4	3.9		3.9	2.3		2.9		0.3			0.3	0.2	
5.7	8.5		3.1	4.3		5.2	4.6	4.4	3.3	3	2.8	0.3	0.3	0.3	0.3	0.3	0.2	
3.6	5.3	5.6	2.5	3.5	3.3	3.2	5.8		2.2			0.3	0.4		0.4	0.3	0.4	
5.8	5.8	6.8	3.4	3.5	4.6	4.1	4.9	6.3	3	2.3	4.5	0.4	0.4		0.2	0.2	0.3	
6.1	6.3	5.3	3.5	3.6	3.8	5	4.6	5	3.4	3.3	3.1		0.4	0.3	0.3	0.4	0.4	
4.9	4.7	6.4	3.7	3.1	3.2	4.3	3.9	6.2	3.5	3.9	3		0.3	0.3	0.3	0.4	0.4	
4.9	5.8	5.6	2.8	2.5	2.9	4.8	6.1		3.1	3.3		0.3	0.3		0.2	0.3	0.4	
2.8	5.5		2.3	3.2		4	5.8		2.5	2.3		0.3	0.3		0.4	0.2		
	6.1			3.2			6.2			2.8						0.4		
	3.7			2.9			4.9			3.1			0.2			0.3		
	6.1			2.9						3.2			0.3			0.5		
	5.1			2.4						2.3			0.3			0.4		
Name	**lkh (b)**	**lkh ©**	**lkh (d)**	**lkv (b)**	**lkv ©**	**lkv (d)**	**rkh (b)**	**rkh ©**	**rkh (d)**	**rkv (b)**	**rkv ©**	**rkv (d)**	**sw (b)**	**sw ©**	**sw (d)**	**iw (b)**	**iw ©**	**iw (d)**
Mean	4.822222	5.569230769	6.042857143	2.944444	3.223077	3.485714	4.3125	5.285	5.233333	2.9125	2.95	3.150	0.316667	0.318182	0.3	0.2875	0.323077	0.3375
Std.Dev	1.050691	1.147830472	0.597272713	0.547948	0.514638	0.637918	0.617328	0.754718	0.888194	0.478115	0.502494	0.623832	0.037268	0.057496	0	0.078062	0.089045	0.085696
95% Conf	0.686439	0.623956287	0.442457687	0.357986	0.279755	0.472567	0.427779	0.467771	0.710690	0.331311	0.311443	0.499161	0.029820	0.033977	#NUM!	0.054094	0.048404	0.059383
Mean	**Std.Dev**	**Mean-1SD**	**Mean+1SD**															
2.878266918	2.033591	0.844676173	4.911857664															